Applied Thermal Engineering 115 (2017) 793–814

Contents lists available at ScienceDirect

Applied Thermal Engineering

journal homepage: www.elsevier.com/locate/apthermeng

Research Paper

Effect of hydraulic diameter and aspect ratio on single phase flow and heat transfer in a rectangular microchannel

Amirah M. Sahar [a,b], Jan Wissink [a], Mohamed M. Mahmoud [a,c,*], Tassos G. Karayiannis [a], Mohamad S. Ashrul Ishak [d]

[a] College of Engineering, Design and Physical Sciences, Brunel University London, UK
[b] Communication Section, University Kuala Lumpur, British Malaysian Institute, Selangor, Malaysia
[c] Faculty of Engineering, Zagazig University, Egypt
[d] School of Manufacturing Engineering, University Malaysia Perlis, Malaysia

ARTICLE INFO

Article history:
Received 18 May 2016
Revised 7 December 2016
Accepted 5 January 2017
Available online 7 January 2017

Keywords:
Aspect ratio
Hydraulic diameter
Microchannels
Single phase flow

ABSTRACT

The effect of aspect ratio and hydraulic diameter on single phase flow and heat transfer in a single microchannel was investigated numerically and the results are presented in this paper. Previously, many studies in literature investigating the effect of geometrical parameters reached contradictory conclusions leaving some phenomena unexplained. Additionally, most researchers studied the effect of channel geometry by varying the channel height for a constant channel width or varying the width for a constant height. This means that the hydraulic diameter and aspect ratio vary simultaneously, which makes it difficult to identify the relative importance of the aspect ratio and the hydraulic diameter. In the present study, the effect of hydraulic diameter was studied by varying the channel width and depth while keeping the aspect ratio constant. The range of hydraulic diameters was 0.1–1 mm and the aspect ratio was fixed at 1. In the second set of simulations, the aspect ratio ranged from 0.39 to 10 while the hydraulic diameter was kept constant at 0.56 mm. The simulations were performed using the CFD software package ANSYS Fluent 14.5. The geometry investigated in this study includes symmetrical cylindrical inlet and outlet plenums and a microchannel. The fluid entered and left the channel vertically from the top in a direction normal to the channel axis. The dimensions of the inlet/outlet plenums (diameter and height measured from the channel bottom surface) were kept constant while the width and depth of the channel were varied. The simulations were conducted for a range of Reynolds numbers (Re = 100–2000) and water was used as the working fluid. A three dimensional thin wall model was used to avoid conjugate heat transfer effects. A constant heat-flux boundary condition was applied at the bottom and vertical side walls of the channel, while the upper wall was considered adiabatic. The friction factor was found to decrease slightly with aspect ratio up to $AR \approx 2$ after which it increased with increasing aspect ratio. The results demonstrated that the slope of the velocity profile at the channel wall changes significantly with aspect ratio for AR > 2. The effect of the aspect ratio and hydraulic diameter on the dimensionless hydrodynamic entry length is not significant. Also, the aspect ratio does not affect the heat transfer coefficient while the dimensionless Nusselt number increases with increasing hydraulic diameter. The friction factor was found to increase with increasing hydraulic diameter.

1. Introduction

1.1. Experimental studies

Understanding fluid flow and heat transfer in microchannels is very important to develop correlations required for the design of microfluidics and heat transfer devices. Several researchers investigated single phase flow and heat transfer in microchannels and reported significant deviations compared to the conventional laminar flow theory. For example, Peng and Peterson [1] investigated the effect of channel size on single phase flow and heat transfer characteristics in microchannels using water and methanol as the test fluids. The channel height was kept constant at 0.7 mm while the channel width was varied from 0.2 to 0.8 mm ($AR = H_{ch}/W_{ch}$ = 0.875–3.5). These dimensions gave a hydraulic diameter (D_h) range of 0.155–0.747 mm. Their experimental results

* Corresponding author at: College of Engineering, Design and Physical Sciences, Brunel University London, UK.
E-mail addresses: mohamed.mahmoud@brunel.ac.uk, mbasuny@zu.edu.eg (M.M. Mahmoud).

http://dx.doi.org/10.1016/j.applthermaleng.2017.01.018
1359-4311/

Nomenclature

AR	aspect ratio, –
A_{ch}	channel cross sectional area, m^2
A_p	plenum cross section area, m^2
A_{ht}	heated area, m^2
C'	constant in Eq. (2)
c_p	specific heat, J/kg K
D_p	plenum diameter, m
D_h	hydraulic diameter, m
f	fanning friction factor, –
f_{app}	apparent friction factor, –
H_{ch}	channel height, m
H_m	manifold height, m
H_p	plenum height, m
h	heat transfer coefficient, W/m^2 K
h_{av}	average heat transfer coefficient, W/m^2 K
$k(\infty)$	constant in Eq. (2)
k_f	fluid thermal conductivity, W/m K
K_c	contraction loss coefficient, –
L_{ch}	channel length, m
L_e	entrance length, m
$\dot{m}$	mass flow rate, kg/s
Nu	Nusselt number, –
Nu_{av}	average Nusselt number, $\frac{h_{av}D_h}{k_f}$, –
$P_{ch,in}$	pressure inlet, Pa
$P_{ch,out}$	pressure outlet, Pa
ΔP_{ch}	channel pressure drop, Pa
ΔP_{ex}	sudden expansion loss, Pa
ΔP_c	sudden contraction loss, Pa
p	pressure, Pa
P_o	pressure outlet, Pa
Pr	Prandtl number, –
Po	Poiseuille number, fRe, –
q''	heat flux, W/m^2
Re	Reynolds number, $\frac{\rho_f V D_h}{\mu_f}$, –
Ra	average roughness, m
T_w	wall temperature, K
T_f	fluid temperature, K
$T_{f,av}$	average fluid temperature, K
$T_{w,av}$	average wall temperature, K
T_i	fluid inlet temperature, K
T_o	fluid outlet temperature, K
V_p	velocity in the manifold, m/s
V_i	velocity inlet, m/s
V_{ch}	velocity inside the channel, m/s
V_{max}	maximum velocity, m/s
V	velocity, m/s
V_P	velocity in the plenum, m/s
v_f	fluid specific volume, m^3/kg
W_{ch}	channel width, m
x, y, z	Cartesian coordinates, m

Greek symbols

μ	viscosity, kg/m s
μ_f	fluid viscosity, kg/m s
ρ	density, kg/m^3
ρ_f	fluid density, kg/m^3

demonstrated that the start of the laminar-to-turbulent flow transition occurs at $Re \approx 300$, while a fully developed turbulent flow regime was first obtained at $Re \approx 1000$. Additionally, the heat transfer coefficient in the channel with aspect ratio 1.75 was found to be much higher than the one obtained in other channels. They did not explain why the heat transfer coefficient is high in this channel compared to the other investigated channels. Peng et al. [2] investigated experimentally flow characteristics of water flowing through rectangular microchannels having a hydraulic diameter range of 0.113–0.367 mm, an aspect ratio range of 0.333–1 and a relative average roughness (Ra/D_h) range of 0.6–1%. The critical Reynolds number for the onset of transition from laminar to turbulent flow was found to depend on the channel hydraulic diameter. Transition occurred at $Re = 200$ for $D_h \leqslant 0.2$ mm and at $Re = 700$ for $D_h \geqslant 0.2$ mm. The friction factor was found to deviate significantly from the conventional laminar flow theory. For example, in the laminar region, the friction factor was found to be proportional to $Re^{-1.98}$ rather than Re^{-1}. Also, the friction factor was found to increase as the aspect ratio (H_{ch}/W_{ch}) increases while it decreased with decreasing hydraulic diameter. It is worth mentioning that the different flow regimes (laminar, transitional and turbulent) were identified from changes in the slope of the friction factor plotted against Re. They attributed this early transition to the significant effect of the channel wall, which influences the intensity of the velocity fluctuations due to inertia and viscous forces. Additionally, they found that the Poiseuille number (Po) increases with increasing aspect ratio, which is contrary to the behaviour in conventional large-diameter channels. However, they reported that it is difficult to explain the effect of aspect ratio due to the narrow range of aspect ratios examined in their study (few experimental data).

Pfund et al. [3] conducted an experimental study to measure the pressure drop directly across a microchannel excluding entrance and exit losses. The test section was designed such that flow visualization was possible in order to detect different flow regimes (laminar, transition and turbulent). The channel width and length were kept constant at 10 mm and 100 mm, respectively, while the channel height was varied from 0.128 to 1.05 mm ($AR = 0.0128–0.105$ and $D_h = 0.025–0.19$ mm). The surface roughness of the examined channels ranged from 0.16 μm to 1.9 μm. The local pressure was measured at eleven equidistance locations along the channel. Water was used as the working fluid. The onset of laminar-to-turbulent flow transition was found to occur at a Re range of 1500–2200, where the lower value corresponds to the smaller channel depth. The Poiseuille number (Po) was found to be significantly higher than the theoretical value for fully developed laminar flow as predicted by Eq. (1) below given by Shah and London [4]. The deviation was found to increase with either decreasing the channel height for the same surface roughness (0.16 μm average roughness) or increasing the surface roughness for the same channel height (1.9 μm average roughness). However, they reported that it is difficult to conclude which parameter (channel geometry or surface roughness) has the strongest effect on the Poiseuille number (Po) due to the experimental uncertainty.

$$Po = 24[1 - 1.3553AR + 1.9467AR^2 - 1.7012AR^3 + 0.9564AR^4 - 0.2537AR^5] \quad (1)$$

Xu et al. [5] investigated single phase pressure drop for water flow in silicon and aluminium microchannels. The hydraulic diameter was varied from 0.03 to 0.344 mm while the aspect ratio was varied

from 0.583 to 24.4. The surface roughness of the aluminium channels was 0.5 μm while that of the silicon channels was 0.02 μm. Based on theoretical analysis, Xu et al. [5] reported that the effect of surface roughness can be ignored for a relative roughness less than 3%. The results demonstrated that there is a good agreement with the laminar flow theory for the silicon channels while significant deviations were found for the aluminium channels for $D_h < 0.1$ mm. The value of the friction factor was found to decrease as the diameter decreases for $D_h < 0.1$ mm and the values were smaller than predicted by the conventional laminar flow theory ($Po = 24$). Additionally, the onset of transition from laminar to turbulent flow in the aluminium channels occurred at $Re = 1500$. They attributted the difference observed in the aluminium channels compared to the silicon channels to deviations in the channel cross sectional area resulting from the difference in the manufacturing method and test section sealing. The aluminium channels were manufactured by machining on aluminium substrate and sealed by a top cover which might create a small gap at the top of the channel. On the contrary, the silicon channels were fabricated by the etching method which is more accurate than machining and the top cover sealed the test section using an anodic bonding technique. Gao et al. [6] investigated single phase flow of water in rectangular microchannels etched in a silicon wafer with a channel height range 0.1–1 mm and a fixed width of 25 mm ($AR = 0.003$–0.04 and $D_h = 0.008$–0.077 mm). The surface roughness was less than 0.1 μm. The results demonstrated that channel height does not have a significant effect on the Poiseuille number in the laminar region where the value was almost constant at about 24 (the fully developed value). Also, the length of the entry region was found to be equal to $0.1ReD_h$. The heat transfer results showed that for a channel height less than 0.4 mm, the Nusselt number decreases with decreasing channel height. However, the dimensional heat transfer coefficient plotted against channel height indicated an opposite effect where the coefficient increased with decreasing channel height, i.e. decreasing D_h. They attributted this behaviour to: (1) possible inappropriateness of using the hydraulic diameter to represent the phenomena at micro scale, (2) electrokinetic effects and (3) the presence of a thin layer of air trapped next to the wall. However, they reported that there is no satisfactory explanation for the results presented in their study. It is worth mentioning that the transition was found to occur at $Re = 3500$–4000.

Zhang et al. [7] studied experimentally the effect of hydraulic diameter and aspect ratio on fluid flow and heat transfer of water in aluminium multiport microchannel flat tubes. The hydraulic diameter was varied from 0.48 mm to 0.84 mm while the aspect ratio was nearly constant ($AR = 0.83$–0.88) and the aspect ratio was varied from 0.45 to 0.88 while the hydraulic diameter was almost constant ($D_h = 0.6$–0.63 mm). The relative roughness of all tested samples ranged from 0.29% to 1.06%. The experiments were performed for Reynolds number ranging from 120 to 3750. They reported that the friction factor for all test samples agrees well with the correlation of Shah and London [4] for fully developed laminar flow and thus they concluded that the effect of entry region is negligible for $L/D_h > 179$. The transition from laminar to turbulent flow was found to occur at $Re = 1200$–1600 without an evidence on the correlation between aspect ration and the early transition from laminar to turbulent flow. Additionally, the aspect ratio was found to have an insignificant effect on heat transfer rate and the reported heat transfer enhancements in their study was attributted to the effect of surface roughness and the entry region.

Contrary to the above studies, some researchers investigated single phase flow and heat transfer in microchannels and reported insignificant deviations compared to the conventional laminar flow theory. Judy et al. [8] conducted an experimental study to measure the single phase pressure drop in circular and square microchannels. The microchannels were fabricated from two different materials namely fused silica and stainless steel. The hydraulic diameter and length of the channels ranged from 0.015 to 0.15 mm and 36 to 300 mm, respectively. All channels were tested using three fluids; distilled water, isopropanol and methanol. No difference in behaviour was found for circular and square channel geometries and the Poiseuille number (Po) was nearly independent of Re for all diameter ranges in the laminar regime. The measured friction factor was in good agreement with the conventional laminar flow theory, without early transition and no significant influences of fluid properties were detected. Mokrani et al. [9] designed an experimental device and investigated fluid flow and convective heat transfer in low aspect ratio ($AR < 0.1$) rectangular microchannels by varying the channel height from 0.05 to 0.5 mm and the hydraulic diameter from 0.1 to 1 mm. They concluded that the conventional laws and correlations are applicable to microchannels with $D_h \geqslant 0.1$ mm. It was also observed that the microchannel hydraulic diameter has no effect on the Nusselt number.

Rosa et al. [10] investigated the scaling effects on single phase flow in microchannels. They concluded that macro scale theory and correlations are valid at micro scale if measurement uncertainty and scaling effects were carefully considered. These scaling effects include: entrance effects, viscous heating, conjugate heat transfer, electric double layer effects, surface roughness, and properties dependent on temperature, compressibility and rarefactions (for gas flow only).

1.2. Numerical studies

Numerical simulations have become an important tool to predict the fluid flow and heat transfer in microchannels. Gamrat et al. [11] performed a 2D and 3D numerical study on the conduction and entrance effects on laminar flow heat transfer of water in rectangular microchannels. They modeled the geometry of the test section used in the experiments conducted by Gao et al. [6] mentioned above for a Re number range 200–3000. The numerical Poiseuille number results was found to be significantly smaller than that predicted by Eq. (2) below given by Shah and London [4] for developing laminar flow. The value of the constants $K(\infty)$ and C' in Eq. (2) depend on channel aspect-ratio and the values are given in Ref. [12]. They attributted this deviation to the boundary layer characteristics at the channel entrance which were not considered in the model of Shah and London [4] who assumed a uniform velocity profile at the channel inlet. Furthermore, the numerical results revealed no significant size effects on heat transfer in the microchannel heat sink down to the smallest size considered in their paper (0.1×25 mm).

$$f_{app}Re = \frac{3.44}{\sqrt{x^+}} + \frac{(f\ Re)_{fd} + \frac{K(\infty)}{4x^+} - \frac{3.44}{\sqrt{x^+}}}{1 + \frac{C'}{(x^+)^{0.2}}}, \quad x^+ = \frac{x}{Re\ D_h} \tag{2}$$

Nowadays, numerous work has been done using Computational Fluid Dynamics (CFD) software packages to predict the flow and heat transfer characteristics in microchannels. In Ansys Fluent, there are two approaches for dealing with the wall boundary. The first approach is called the *full conjugate model* in which the solid and fluid zones are meshed and the energy equation is solved in both zones. Thus, the heat conduction in all directions is accounted for through solving the energy equation in the solid and the fluid. The second approach is a simplified approach called the *thin-wall model*. Here the solid zone heat transfer is modeled by a constant heat flux at the outer surface of the walls of the fluid zone. As there is no need to calculate heat transfer in the solid zone the numerical calculation time is reduced. Fig. 1 depicts the difference between the two approaches. The *thin wall model* approach is illustrated in Fig. 1(a) while Fig. 1(b) shows the *fully conjugate model* that includes the entire substrate. Lee et al. [13] conducted

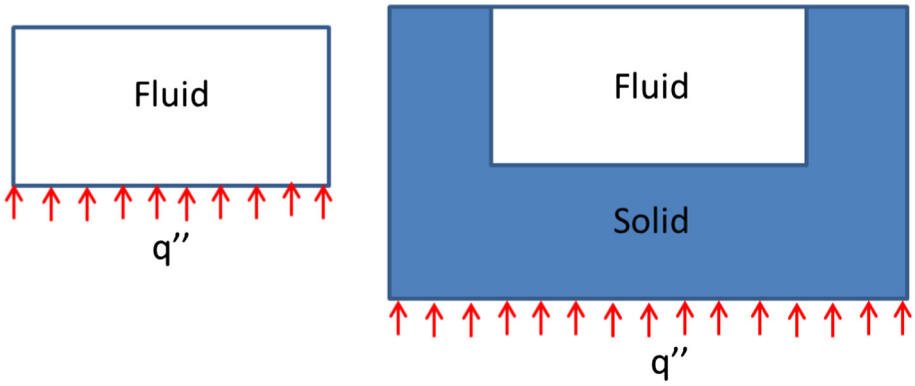

Fig. 1. Schematic of (a) thin wall model and (b) conjugate model.

experimental and numerical studies to investigate the validity of the classical laminar flow theory at micro scale level. The investigated channels were made of copper and have a rectangular cross sectional area and a hydraulic diameter range of 0.318–0.903 mm and a length of 24.5 mm. They evaluated two numerical models, namely a *fully conjugate model* and a *thin-wall model*. In the *fully conjugate model*, both convection in the channel and conduction in the substrate were taken into account. The substrate thickness of 1.5 mm was included in this model and a uniform heat-flux was applied at the bottom surface, simulating the heat flow from the cartridge heaters. For a thin wall analysis, a thin and highly conductive wall without axial conduction was employed in this model. Utilizing symmetry conditions, only a quarter domain was modeled. Their results showed that there is no significant difference between the predictions made by the two models and the experimental data, i.e. insignificant conjugate effects. Thus, they concluded that the *thin-wall model* can be used as a computationally economical alternative to the *fully 3D conjugate* analysis. Recently, a numerical study on single phase flow and heat transfer in microchannels was conducted by Sahar et al. [14]. They examined the following models: *2D thin-wall* heated from the bottom, *3D thin-wall* heated from the bottom, *3D thin-wall* heated from three sides and *3D fully conjugate model*. The numerical predictions were compared with experimental data. In all *thin wall model* simulations, the thermal boundary conditions are applied at the outer surface of the wall (at the solid-fluid interface). For the 3D fully conjugate model, the full copper block, similar to the one used in the experiment, was simulated. A constant heat flux boundary condition was applied at the location of the cartridge heater. They found that conjugate effects were significant and the uniform heat flux assumption was not valid. Accordingly, the experimental results deviated from the *3D fully conjugate* model. The deviation was attributed to the conjugate effect, where the heat flux was not uniformly distributed along the channel. In order to examine this behaviour, they conducted the simulation at conditions similar to those assumed in the experimental data reduction (*3D thin wall* model) and found excellent agreement with the experimental data. It is worth mentioning that the *3D thin wall* model and the experimental data shared the inaccurate or erroneous assumption of uniform heat flux boundary conditions along the channel walls. The insignificant conjugate effects reported by Lee et al. [13] could be attributted to the fact that the substrate thickness used in their *3D full conjugate* model was 1.5 mm which is very small compared to the copper block thickness used in Sahar et al. [14], which is 24 mm.

Moharana and Khandekar [15] conducted a numerical study on axial wall heat conduction in simultaneously developing flow in rectangular microchannels using water at $Re = 100$. They conducted four sets of simulations which are summarized as follows: (1) varying the channel aspect ratio while keeping the channel cross-sectional area constant, (2) varying the channel aspect ratio but keeping the heated perimeter constant, (3) varying the channel aspect ratio but keeping the channel width constant and (4) varying the channel aspect ratio while keeping the channel height constant. The channel aspect ratio was varied from 0.25 to 2.22 and the hydraulic diameter varied from 0.16 to 0.203 mm. A constant heat flux boundary condition was applied at the bottom of the channel substrate while all other surfaces were considered adiabatic. They found that the average Nusselt number decreases with increasing aspect ratio (W/H) until $AR \approx 2$ after which it starts to increase with aspect ratio for constant cross sectional area and heating perimeter of the channel. The authors did not give an explanation to this phenomenon. Accordingly, they suggested using channels of $AR > 2$ for better heat transfer performance and ease of manufacture, compared to channels of low aspect ratio. Dharaiya and Kandlikar [16] conducted numerical investigations of heat transfer in rectangular microchannels under uniform circumferential and axial heat flux boundary conditions in fully developed and developing flow. The aspect ratio was varied from 0.1 to 10 with the length of channel was 100 mm. Five different cases were simulated under uniform wall heat flux; (1) four sides heated, (2) three sides heated, (3) two sides heated (opposing walls), (4) two sides heated (adjacent walls), and (5) one side heated. The effect of the inlet plenum was studied through simulating a channel with a plenum that has an abrupt decrease in the cross sectional area and another plenum with a gradual decrease in cross sectional area. It was found that the entrance effects on *Nu* in the entry region of the developing flow are insignificant. Also, in the fully developed region, *Nu* was found to reach an asymptotic value and increases with increasing aspect ratio for the four and three sides heated boundary conditions. For the one side and two sides heated boundary conditions *Nu* was found to decrease with aspect ratio. Additionally, the thermal entrance length was found to increase as the aspect ratio increases.

Gunnasegaran et al. [17] studied numerically the effect of channel shape on water flow and heat transfer in multi-microchannel configurations for $Re = 100–1000$. They studied three different geometrical shapes namely; rectangular, trapezoidal and triangular. For the rectangular geometry, three cases were investigated with hydraulic diameter 0.259–0.385 mm and aspect ratio (H_{ch}/W_{ch}) range 1.03–2.56. They reported that the rectangular channel with the smallest hydraulic diameter has the highest heat transfer coefficient. Also, the heat transfer coefficient and the Poiseuille number were higher compared to the other examined geometries. It was found also that the Poiseuille number increases as the aspect ratio increases. Wang et al. [18] conducted a similar numerical study

investigating the effect of channel shape on fluid flow and heat transfer in multi-microchannel configurations. Twelf heat sinks with rectangular channels having hydraulic diameter range 0.172–0.406 mm and aspect ratio range 1.03–20.33 were investigated. The overall thermal resistance and pumping power were used as evaluation parameters. They reported that the rectangular geometry achieved the best performance for aspect ratio range 8.904–11.442 and the rectangular geometry achieved the lowest thermal resistance compared to the triangular and trapezoidal geometries. On the other hand, the pressure drop was found to increase with *Re* and *AR*. This means that increases in *Re* or *AR* will raise pumping power consumption. Therefore, they suggested that a smaller D_h combined with a larger wetted perimeter and convective heat exchange area in a rectangular microchannel is beneficial for improving the cooling performance of microchannel heat sinks.

1.3. Hydrodynamic entry length

Recently, some researchers such as [19,20] investigated the scaling effects on the hydrodynamic entrance length. Ahmad and Hassan [19] carried out an experimental investigation to study the hydrodynamics in the entrance region of microchannels using microparticle image velocimetry (micro-PIV). The experiments were performed in the laminar flow region with a *Re* number range of 0.5–200. Square microchannels with hydraulic diameters of 0.5 mm, 0.2 mm and 0.1 mm were used and the aspect ratio effect was not considered. They indicated that for $Re > 10$, the scaling effect (channel size) on the entrance length was insignificant and the dimensionless entry length (L_e/D_h) depends only on *Re*. Thus, they proposed a general empirical correlation for macro and microchannels to estimate the dimensionless entry length, as given by Eq. (3) below.

$$\frac{L_e}{D_h} = \frac{0.60}{0.14Re + 1} + 0.0752Re \tag{3}$$

Galvis et al. [20] investigated numerically the effect of aspect ratio and hydraulic diameter on the hydrodynamic entrance length in rectangular microchannels. The numerical simulations were performed to evaluate the effect of *Re* number ($50 < Re < 200$), hydraulic diameter ($0.1\ \text{mm} < D_h < 0.5\ \text{mm}$) and channel aspect ratio ($1 < AR < 5$) on the entrance length in rectangular microchannels. They reported that the channel aspect ratio has insignificant effect on the dimensionless entrance length for $Re > 50$. New correlations were proposed to predict the entrance length for rectangular microchannels with $1 < AR < 5$ and for $Re < 50$.

$$\frac{L_e}{D_h} = \frac{0.740}{0.09Re + 1} + 0.0889Re; \quad AR = 1.0 \tag{4}$$

$$\frac{L_e}{D_h} = \frac{0.715}{0.115Re + 1} + 0.0825Re; \quad AR = 1.25 \tag{5}$$

$$\frac{L_e}{D_h} = \frac{1}{0.098Re + 1} + 0.9890Re; \quad AR = 2.50 \tag{6}$$

$$\frac{L_e}{D_h} = \frac{1.1471}{0.034Re + 1} + 0.0818Re; \quad AR = 5.0 \tag{7}$$

The above review demonstrates that there are many studies investigated the effect of geometrical parameters in rectangular channels and reported contradicting results. In most studies, the effect of channel geometry was investigated by varying the channel height for a fixed channel width or vice versa. This means that the hydraulic diameter and aspect ratio vary simultaneously, which makes it difficult to identify the relative importance of the aspect ratio and the hydraulic diameter. This could be a possible factor explaining some discrepancies reported in literature. Additionally, some researchers such as [6] reported that the hydraulic diameter may not be the appropriate geometrical parameter to describe flow and heat transfer in microchannels. Thus, the present numerical study examined this factor and the effect of hydraulic diameter was investigated by keeping the channel aspect ratio constant while the effect of aspect ratio was investigated by keeping the hydraulic diameter constant. The geometry investigated in this study includes inlet and outlet plenums, which are very similar to the geometry investigated in many flow boiling fundamental studies, i.e. flow boiling in a single channel. It is known that single phase heat transfer coefficient and friction factor are commonly used in the evaluation of flow boiling heat transfer and pressure drop models and correlations. The associated entry and exit pressure losses are also evaluated in the present study, which are usually needed for the deduction of the two phase pressure drop across the channel. This research contributes to the understanding of the effect of each geometric parameter, which is important from a fundamental and a design point of view.

2. Model description

The description of the model used in the present numerical investigation will discuss in this section. The geometry investigated in this study includes symmetrical cylindrical inlet and outlet plenums (8 mm height and 2 mm diameter) and a rectangular microchannel. The fluid entered and left the channel vertically from the top in a direction normal to the channel axis. The dimensions of the inlet/outlet plenums (diameter and height measured from the channel bottom surface) were kept constant in this study while the width and height of the channel were varied, see Fig. 2. In order to understand the effect of hydraulic diameter and aspect ratio, the effect of other parameters such as conjugate effects should be eliminated. Accordingly, the 3D thin-wall model that ignores the conjugate effects was used in this study. A constant heat flux boundary condition was applied at the bottom wall and both vertical side walls of the channel, while the upper channel wall was considered adiabatic. This simulates the boundary conditions encountered in several flow boiling studies when there is a glass window on the upper side for flow visaulization. The same heat flux was applied at the three heated walls for all tested channels in the present study. At the inlet plenum, a uniform velocity was prescribed, and a zero static pressure was employed at the outlet plenum. Since laminar flow is the dominant flow regime in microchannels, the simulation was conducted for a range of *Re* number between 100 and 2000 and water was used as the working fluid. In the first set of simulations, the hydraulic diameter was varied from 0.1 to 1 mm while the aspect ratio was kept constant at 1. In the second set of runs, the aspect ratio was varied from 0.39 to 10 while the hydraulic diameter was kept constant at 0.56 mm, see Table 1.

The simulation was conducted using FLUENT 14.5, while ICEM 14.5 was used to design the geometrical models, produce the grid generation and set the boundary definitions. The SIMPLE scheme is used to resolve the pressure-velocity coupling. The flow momentum and energy equations are solved with a first-order upwind scheme. The simulations are performed using a convergence criterion of 10^{-6}. The hexa meshing grid scheme was used to mesh the system as shown in Fig.3. A highly compressed non-uniform grid near the channel walls was adopted in order to properly resolve viscous shear layers. Grid nodes were also concentrated along the axial direction in the entrance of the channel in order to properly resolve the flow and thermal development regions as adopted by Fedorov and Viskanta [21] and Qu and Mudawar [22]. A grid dependency study was conducted using the axial Nusselt number (see Fig. 4) as a criterion to ensure the results are independent of

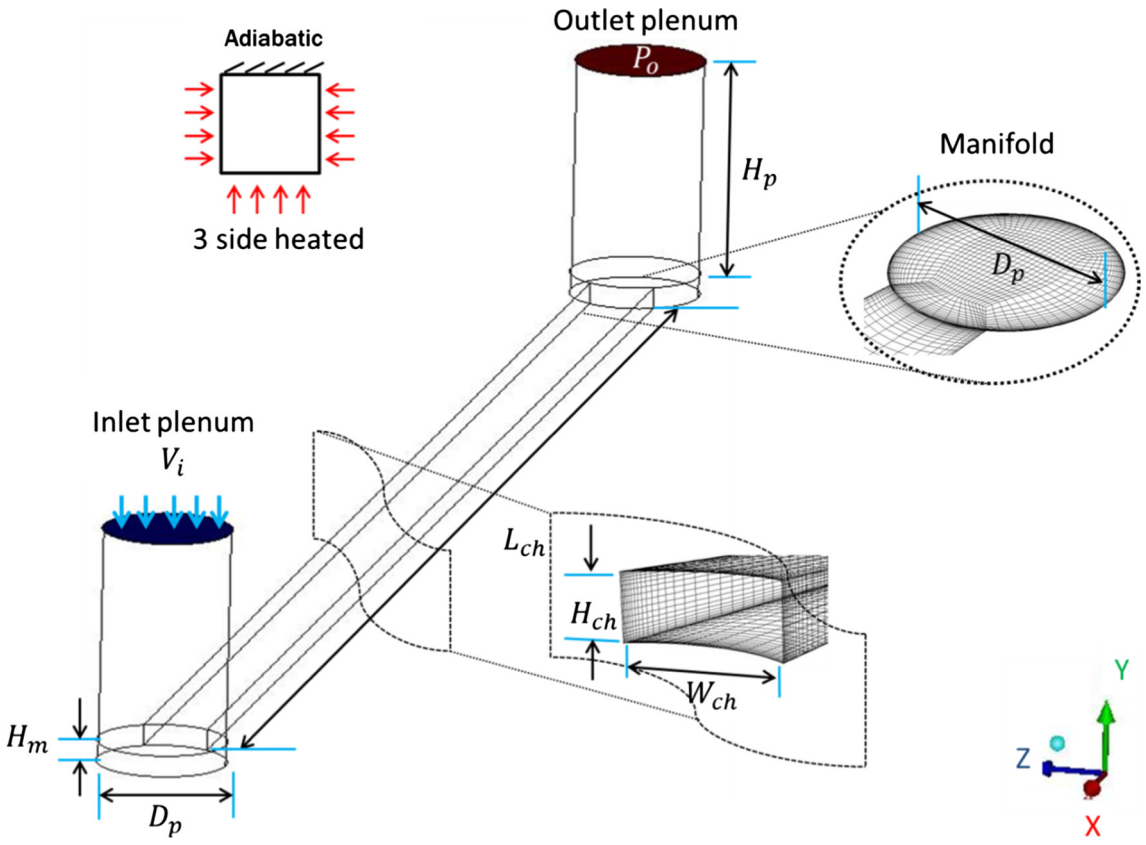

Fig. 2. 3D Thin wall computational model ($H_{ch} = H_m$).

Table 1
Channel dimensions used for the numerical simulations in the present study, $L_{ch} = 62$ (mm).

Run	W_{ch} (mm)	H_{ch} (mm)	D_h (mm)	AR (H_{ch}/W_{ch})
1	1	0.39	0.56	0.39
2	0.56	0.56	0.56	1
3	0.46	0.7	0.56	1.52
4	0.42	0.84	0.56	2
5	0.35	1.4	0.56	4
6	0.32	2.4	0.56	7.50
7	0.31	3.1	0.56	10
8	0.1	0.1	0.10	1
9	0.3	0.3	0.3	1
10	0.5	0.5	0.50	1
11	0.7	0.7	0.7	1
12	0.9	0.9	0.9	1
13	1	1	1	1

the mesh. Three different grid sizes of $15 \times 15 \times 300$ (Grid 1), $20 \times 15 \times 400$ (Grid 2) and $20 \times 50 \times 600$ (Grid 3) were used for x-y-z direction representing width, height and length, respectively. Grid sensitivity study was conducted in the laminar and the predicted Nusselt number changed by less than 1% from the $15 \times 15 \times 300$ to the $20 \times 50 \times 600$ grid size. Hence the intermediate grid size of $20 \times 15 \times 400$ was chosen in order to save computational time.

The following assumptions were adopted: (1) steady state fluid flow and heat transfer, (2) incompressible fluid, and (3) negligible radiative heat transfer. Based on these assumptions, the governing differential equations used to describe the fluid flow and heat transfer in the microchannel are given as:

Conservation of mass (continuity)

$$\nabla(\rho \vec{V}) = 0 \tag{8}$$

Conservation of momentum

$$\vec{V} \cdot \nabla(\rho \vec{V}) = -\nabla p + \nabla \cdot (\mu \nabla \vec{V}) \tag{9}$$

Conservation of energy for fluid

$$\vec{V} \cdot \nabla(\rho c_p T_f) = \nabla \cdot (k_f \nabla T_f) \tag{10}$$

The aspect ratio (AR) and hydraulic diameter (D_h) of a rectangular microchannel are defined as:

$$AR = \frac{H_{ch}}{W_{ch}}, \quad Dh = \frac{4(H_{ch} W_{ch})}{2(H_{ch} + W_{ch})} \tag{11}$$

The Reynolds number is defined as:

$$Re = \frac{\rho_f V_{ch} D_h}{\mu_f} \tag{12}$$

The Fanning friction factor is defined as:

$$f = \frac{\Delta P_{ch} D_h}{2 L_{ch} \rho_f V_{ch}^2} \tag{13}$$

and $\Delta P_{ch} = P_{ch,in} - P_{ch,out}$

The local heat transfer coefficient is defined as:

$$h(x) = \frac{q''}{T_{w,av}(x) - T_{f,av(x)}} \tag{14}$$

$T_{w,av}(x)$ is the axial wall temperature calculated by averaging all values obtained by extracting the data using a line plotted along the width and height of the channel at each axial location. $T_{f,av}$(x) is the axial fluid temperature calculated by averaging the data along a line plotted across the width and height of the channel at the centerline of the channel for each axial location. This approached have been compared with the 'mixing cup' temperature, which was usu-

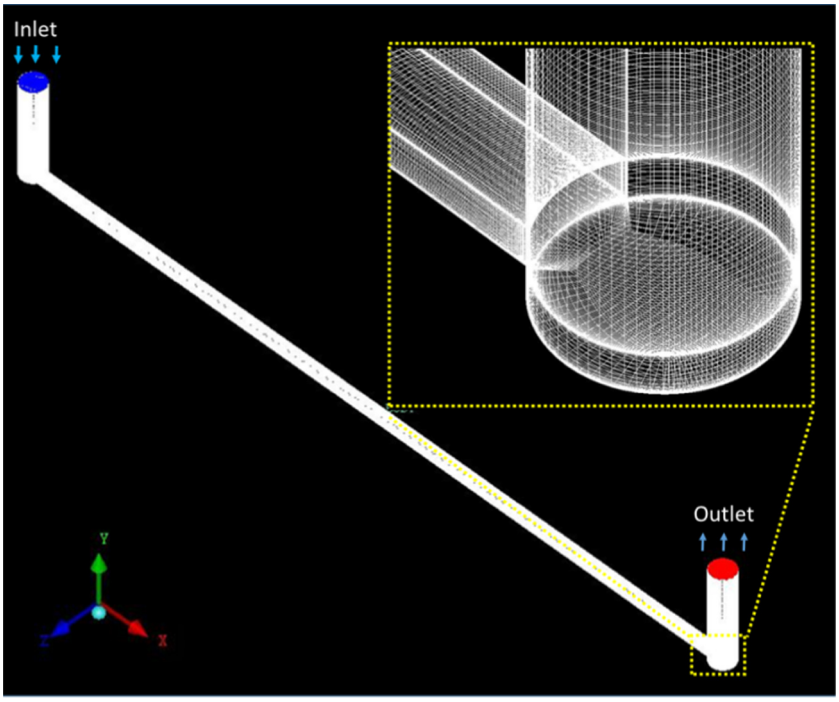

Fig. 3. Schematic and computational meshes of geometrical model.

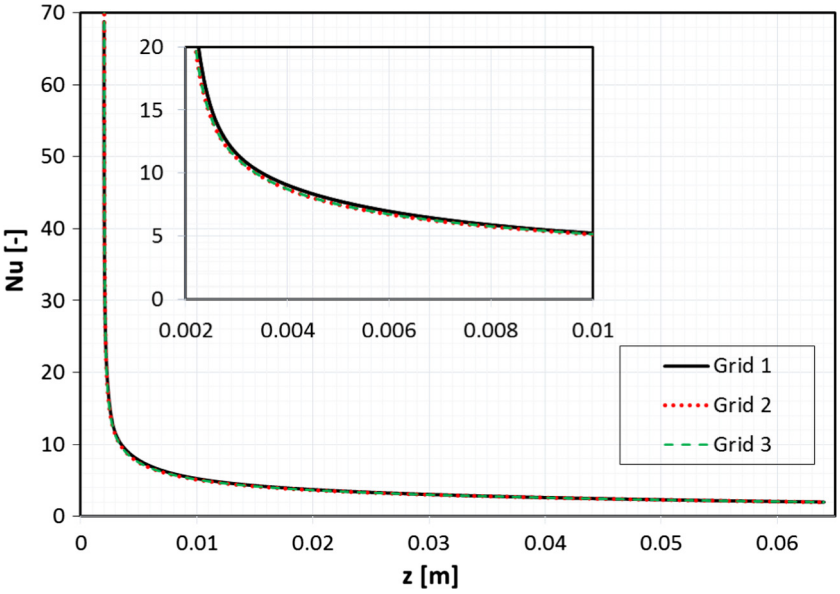

Fig. 4. Grid independence test study for geometrical model.

ally taken as the average fluid temperature and the difference between the two approaches was less than 1%.

The local Nusselt number is defined as:

$$Nu(x) = \frac{h(x)D_h}{k_f} \tag{15}$$

The average heat transfer coefficient is defined as:

$$h_{av} = \frac{1}{L_{ch}} \int_0^{L_{ch}} h(x)dx \tag{16}$$

and the average Nusselt number is defined as:

$$Nu_{av} = \frac{h_{av}D_h}{k_f} \tag{17}$$

3. Results and discussion

This section presents and discusses the numerical results of the effect of aspect ratio and hydraulic diameter on single phase flow and heat transfer in single rectangular microchannels. Section 3.1 presents the validation of the numerical results. Sections 3.2 and 3.3 presented, respectively, the effect of aspect ratio and hydraulic diameter on the hydrodynamic entry length, friction factor and

average Nusselt number. The thermal entry length is not included in this study because the channel is not long enough and the flow is hydrodynamically developed, but thermally developing for all examined conditions. Fig. 5 illustrates the flow development along the channel for $AR = 10$ and $AR = 0.39$ showing that the flow is hydrodynamically developed but thermally developing. At the

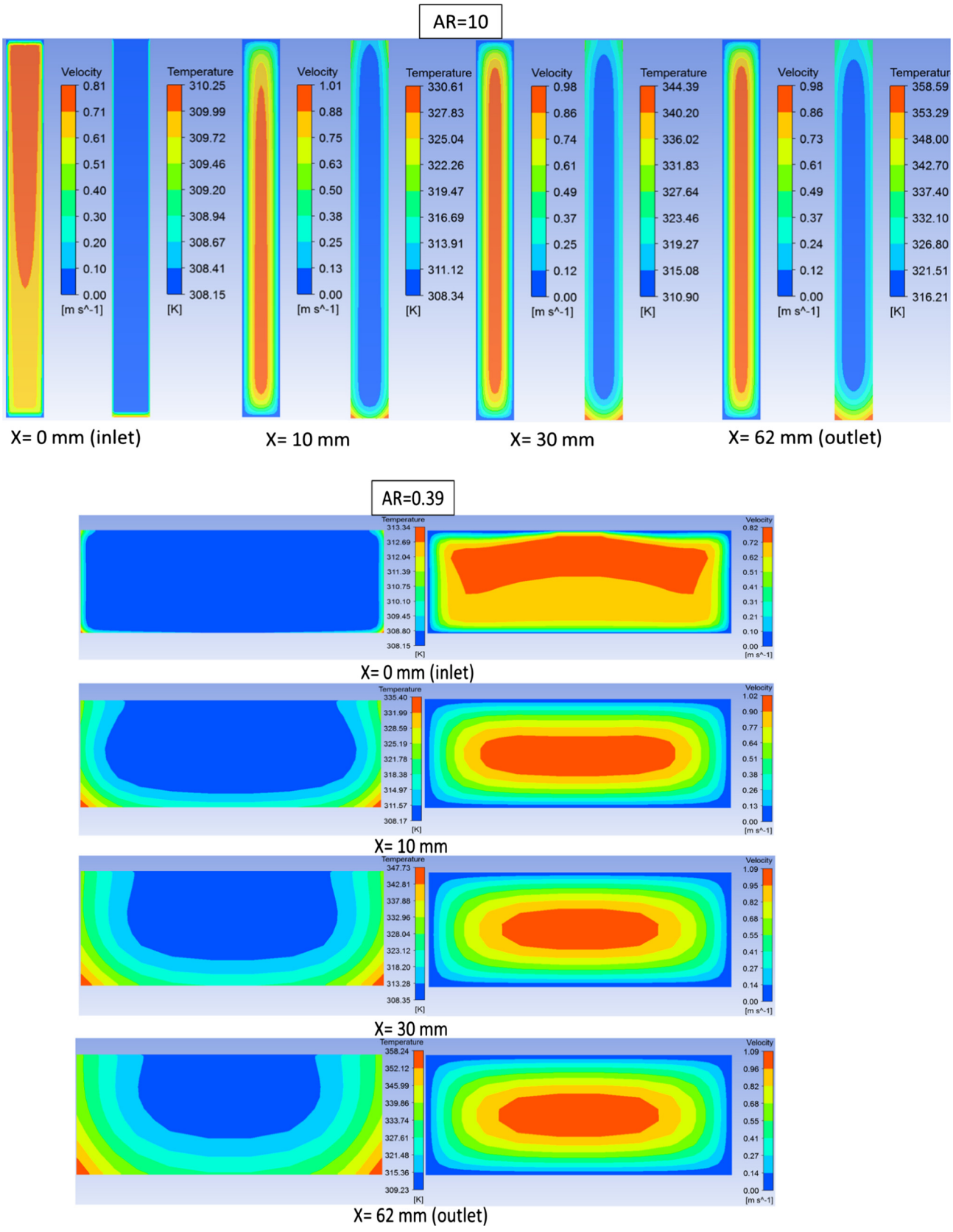

Fig. 5. Velocity and temperature contour at AR = 10 and AR = 0.39 along the channel.

end, the minor losses (entry and exit losses) are discussed in Section 4.

3.1. Validation of numerical results

The numerical results of friction factor and Nusselt number were validated using experimental data obtained using water flow in a single rectangular channel of 0.56 mm hydraulic diameter, 0.39 mm depth and 1 mm width (Run 1 in Table 1). The design of the test section was such that the fluid enters and leaves the channel in a similar way to the configuration depicted in Fig. 2. The details of this validation can be found in Sahar et al. [14]. Fig. 6a shows the heat transfer validation where the predicted average Nusselt number was compared with the experimental data [23], the predictions from the correlations of Shah and London [4] for fully developed and developing flow and the correlation of Bejan [24] for developing laminar flow. It can be seen that the numerical predictions are in excellent agreement with the experimental data. The deviation between the numerical predictions and the predictions from the correlations of Shah and London [4] and Bejan [24] could be due to the fact that these correlations were based on 2D analysis and the effect of the inlet manifold was not included, i.e. they assumed uniform velocity at the channel inlet. Fig. 6b shows the validation of the numerical results of the friction factor using the experimental data [23] and Shah and London [4] correlations for developing and fully developed flow. It is obvious that the numerical results agree very well with the experimental data and mostly also with the correlation of Shah and London [4] for developing laminar flow. The slight deviation from the correlations for both developing and developed turbulent flow observed for $Re > 1400$ might be explained by the flow becoming transitional leading to an increase in friction factor.

3.2. Effect of aspect ratio

3.2.1. Hydrodynamic entry length

The effect of aspect ratio on the dimensionless hydrodynamic entry length (L_e/D_h) is investigated for an aspect ratio range of 0.39–10 and $D_h = 0.56$ mm. The entry length (L_e) can be defined as the length from the channel inlet to the location at which the

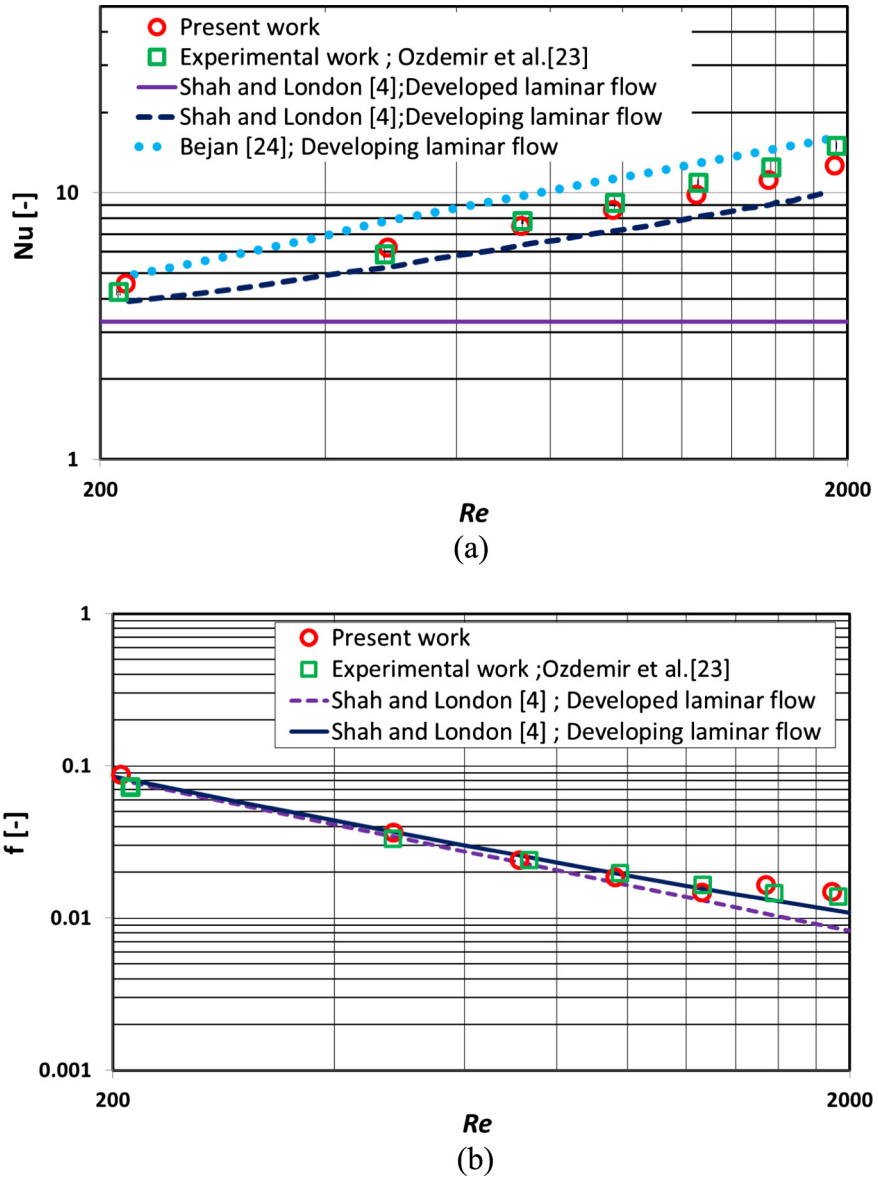

Fig. 6. Comparison of (a) Nusselt number and (b) friction factor with the experimental data [23] and the predictions from correlations, [4,24].

velocity attains 99% of its fully developed value [4]. Fig. 7a depicts an example on how the entry length was obtained in the present study for Re = 235, 591, 873 and D_h = 0.1 mm while Fig. 7b shows how the velocity profile develops along the channel until it reaches the fully developed shape for AR = 0.39 and Re = 181. The numerical data were compared with Eq. (3) proposed by Ahmad and Hassan [19] and Eq. (4) given by Galvis et al. [20] for the dimensionless hydrodynamic entry length. It is worth mentioning that Galvis et al. [20] proposed four different correlations (see Section 1) and each correlation is valid for a certain aspect ratio and Re < 50. They reported that for Re > 50 the effect of aspect ratio on the dimensionless entry length is insignificant and any of the four correlations (Eqs. (4)–(7)) can be used. Thus, Eq. (4) was selected for comparison with the results of the current study. Fig. 8 shows the effect of aspect ratio on the dimensionless hydrodynamic entry length (L_e/D_h) compared to the predictions from Eq. (3) given by Ahmad and Hassan [19] and Eq. (4) given by Galvis et al. [20].

As seen in the Fig. 8, the aspect ratio does not have a significant effect on the dimensionless hydrodynamic entry length and the numerical results are in reasonable agreement with Ahmad and Hassan [19] (the mean absolute error ranged from 1.527% to 24.059%) and Galvis et al. [20] (the mean absolute error ranged from 1.008% to 23.659%). Although the two correlations give a similar range for the mean absolute error, the average value of the mean absolute error from the correlation of Galvis et al. [20] is smaller than that from the correlation of Ahmad and Hassan [19] (7.63% versus 13.6%). These small deviations could be due to differences in entry conditions. It is worth mentioning that in the numerical study of Galvis et al. [20], the velocity was assumed to be uniform at the channel inlet while in the present study the velocity was assumed uniform at the inlet of the plenum. In the

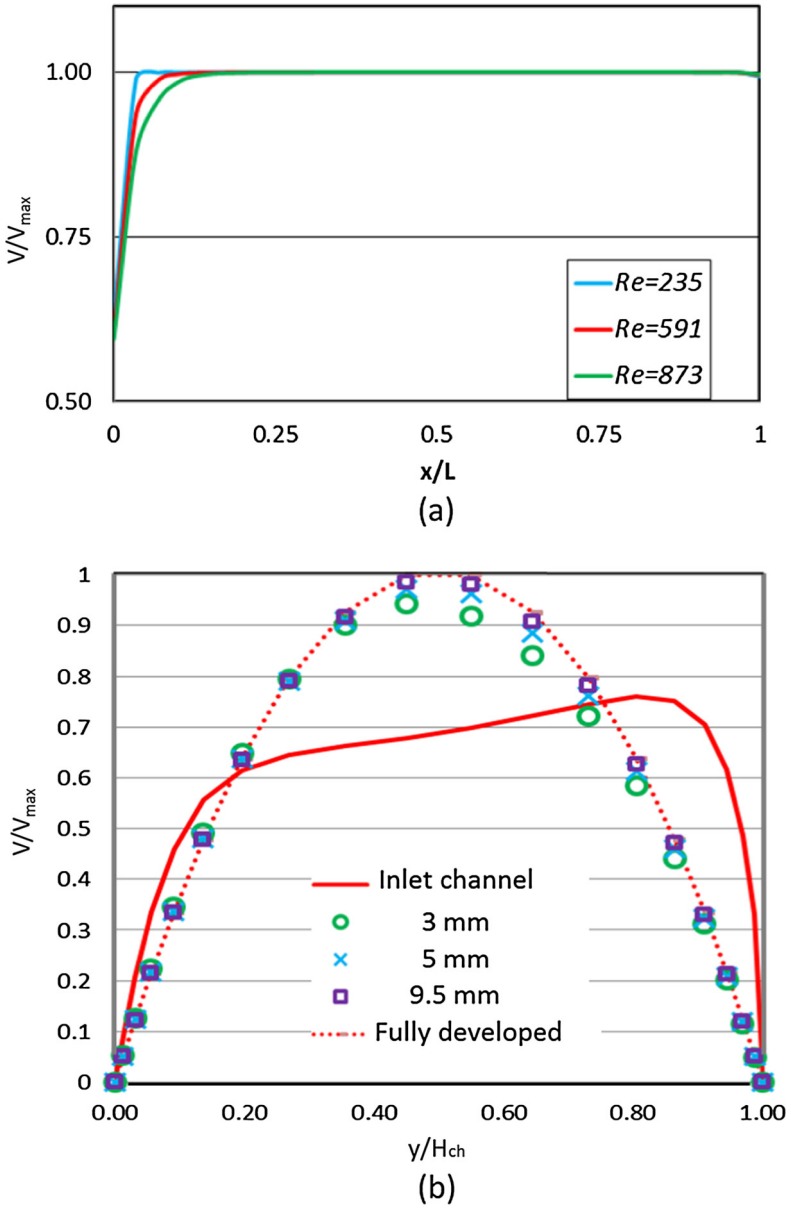

Fig. 7. Hydrodynamic entry length identification, (a) maximum velocity attains 99 % of the fully developed value for D_h = 0.1 mm, (b) development of the velocity profile for Re = 181, D_h = 0.56 mm and AR = 0.39.

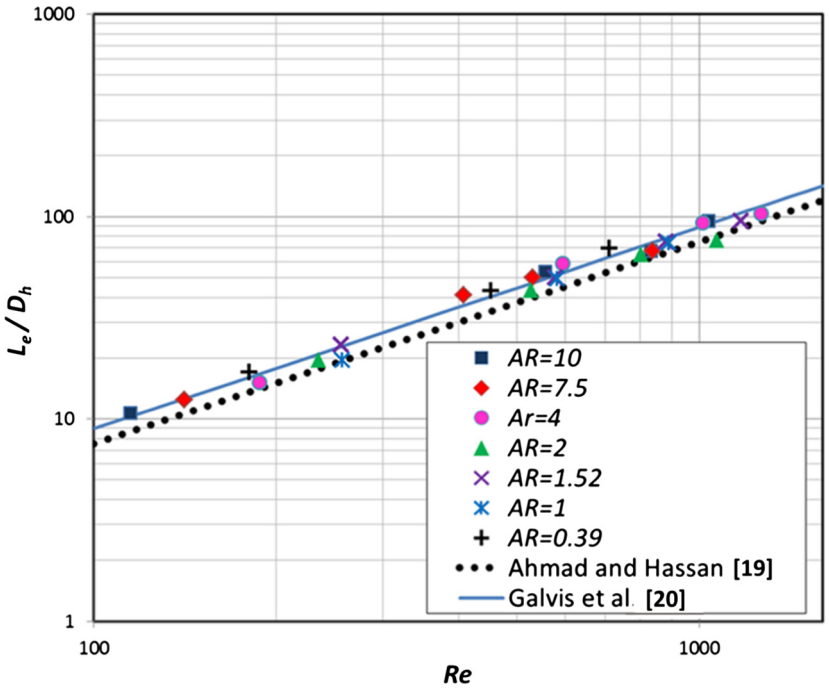

Fig. 8. Comparison of numerical dimensionless entrance length and existing correlations [19] and [20] at different channel aspect ratio ($0.39 < AR < 10$) with $D_h = 0.56$ mm.

experimental study of Ahmad and Hassan [19], the test section consisted of a planar large reservoir (plenum) which was 100 times greater and deeper than the microchannel hydraulic diameter only in the upstream side. On the contrary, in the present study, symmetrical cylindrical inlet and outlet plenum were allocated at the upstream and downstream of the microchannels for all tested channels as shown in Fig. 2. Also, the channels in the present study were simulated with a sharp edge corner at the inlet of the microchannel. This produced a flow separation or vena contracta effect in the inlet region of the microchannel, as shown in Fig. 9.

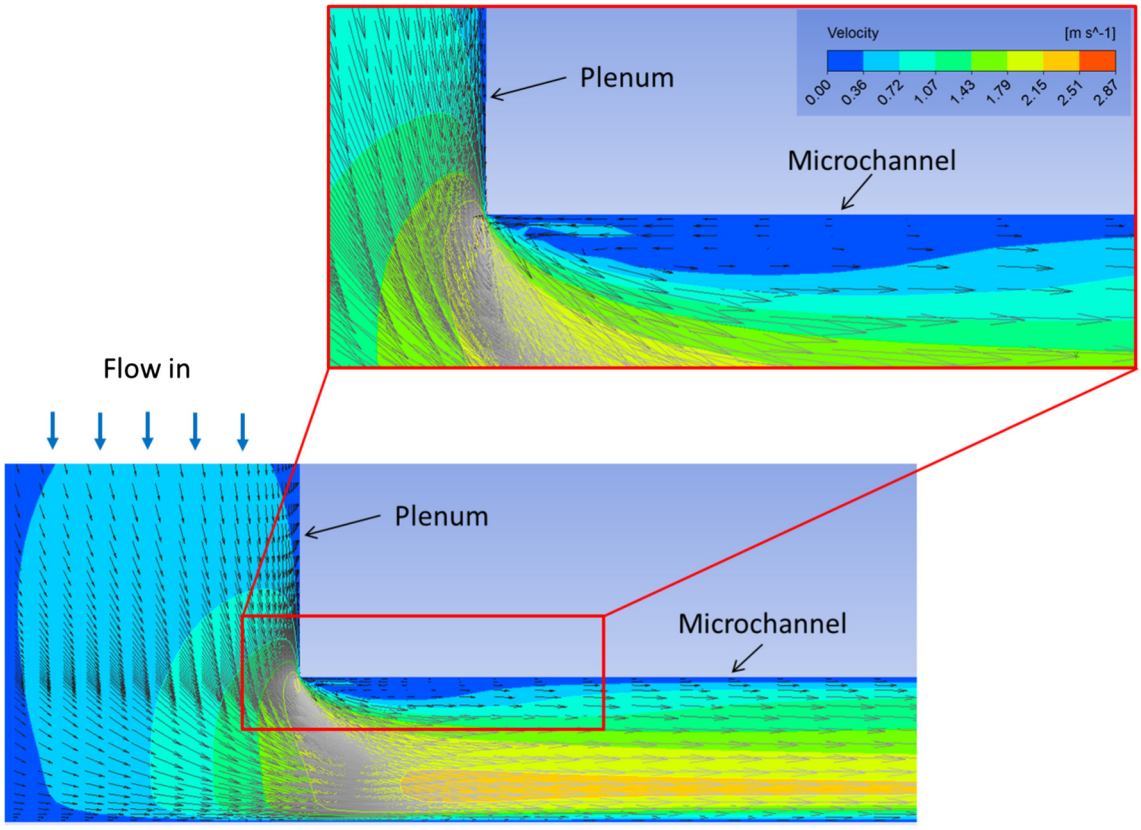

Fig. 9. Vena contracta effects produced by sharp edge corner at the microchannel inlet.

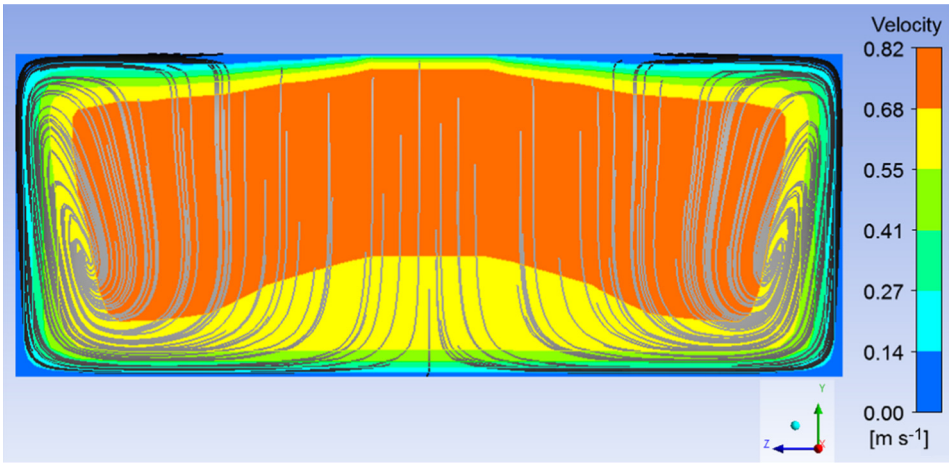

Fig. 10. Velocity contour and streamline at inlet channel.

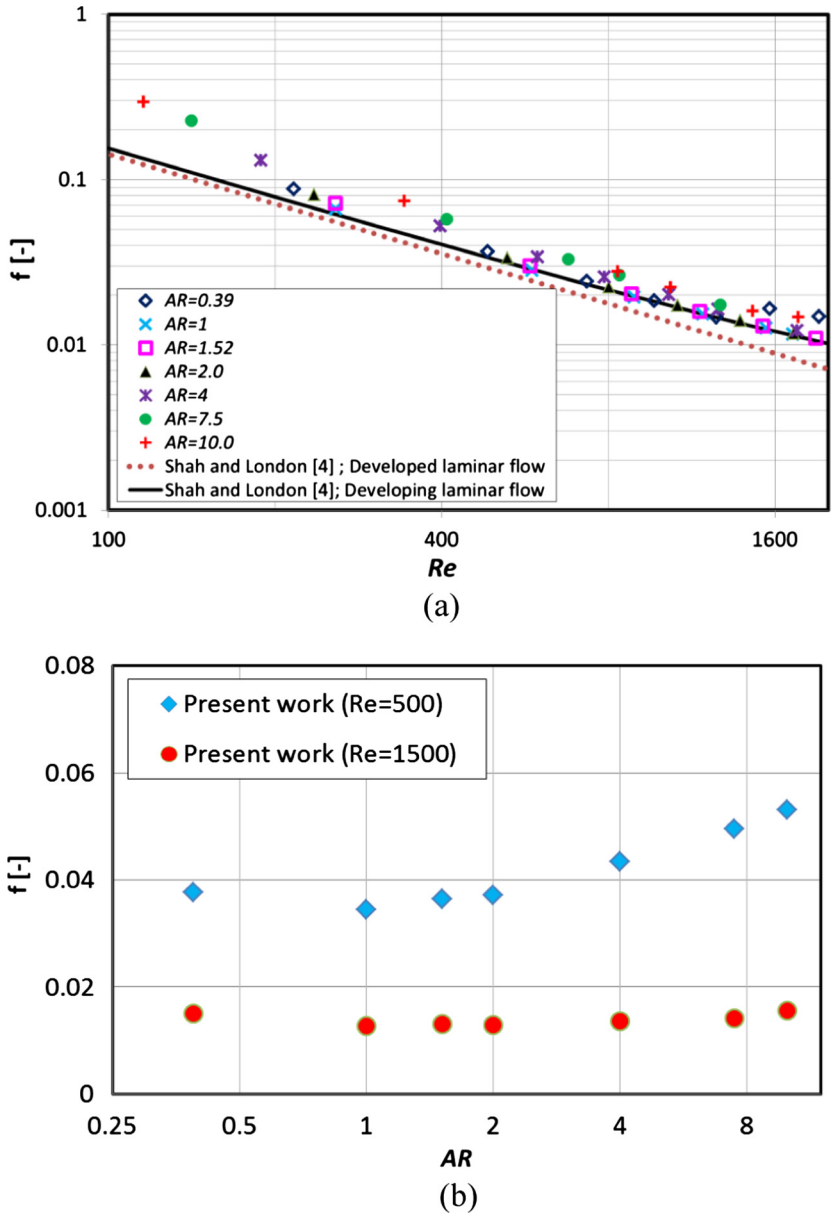

Fig. 11. (a) Comparison between predicted friction factor and existing correlations [4]. (b) Variation of friction factor with varying channel aspect ratio.

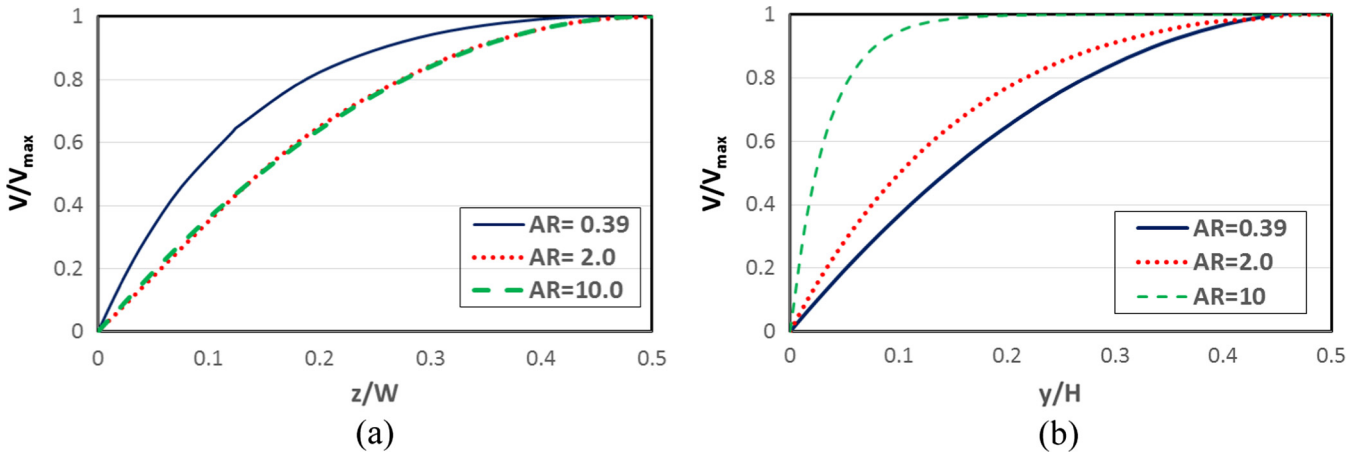

Fig. 12. Fully developed velocity profile against channel height and width for AR = 0.39, 2 and 10 at $Re \approx 500$.

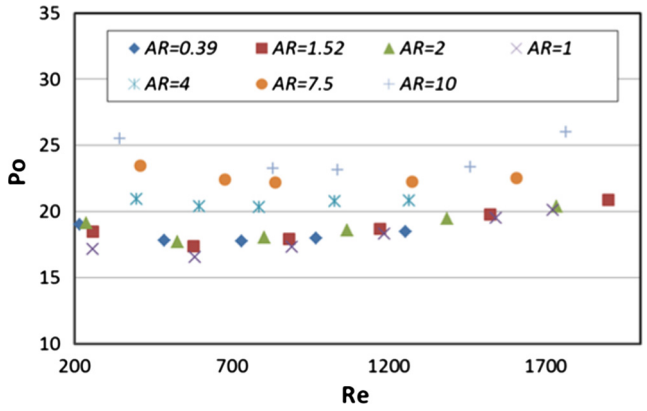

Fig. 13. Effect of Reynolds number and aspect ratio on Poiseuille number.

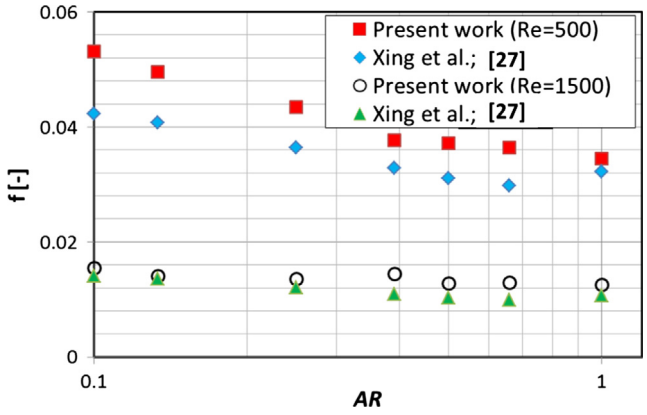

Fig. 14. The friction factor versus aspect ratio compared to the results of Xing et al. [27].

The vena contracta effect was observed only at the corner formed by the top wall and the plenum wall. On the contrary, a non-symmetric vena contracta was observed at the top and bottom wall of the channel in the study of Ahmad and Hassan [20] due to the presence of deeper inlet plenum. Fig. 10 illustrates the velocity streamline at the channel inlet where vortices exists near the side walls. This phenomenon was due to the flow separation at the channel inlet when the flow enters the microchannel from the plenum as stated in [25]. Therefore, the inlet velocity profile needs to be carefully considered in order to estimate the entrance length. As reported by Beavers et al. [26], the inlet velocity profile is dependent on the geometry of the transition section between the plenum and the channel.

3.2.2. Friction factor

Fig. 11 illustrates the effect of aspect ratio on the friction factor for a fixed hydraulic diameter value of 0.56 mm. The numerical results are compared with the correlations proposed by Shah and London [4] for fully developed and developing flow. Fig. 11a demonstrates that for aspect ratio values from 0.39 to 2, there is no significant effect on the friction factor and the trend and magnitudes are very close to the prediction from the correlation of Shah and London [4] for developing flow. For aspect ratios greater that 2, the magnitude of the friction factor and the slope of the line are higher than those predicted using the Shah and London correlation, particularly in the low *Re* number region ($Re < 400$). Fig. 11b shows the friction factor plotted versus aspect ratio for $Re = 500$ and 1500. It can be seen in the figure that the magnitude of the friction factor remains almost constant with increasing aspect ratio up to $AR = 2$, then the values start to increase slightly with aspect ratio for $Re = 500$ and, finally, increase significantly with aspect ratio for $Re = 1500$. The friction factor increased by 10.7% for $Re = 500$ and increased by 36.24 % for $Re = 1500$ when the aspect ratio was increased from 2 to 10. In other words, for design purposes, the aspect ratio should be less than 2 in order to achieve a low pressure drop and, consequently, pumping power. The effect of aspect ratio on the friction factor can be explained by plotting the fully developed velocity profile along the channel height and width as seen in Fig. 12 for the lowest aspect ratio ($AR = 0.39$), for aspect ratio = 2 and for the highest aspect ratio ($AR = 10$). Fig. 12 indicates that there is a small change in the slope of the velocity profile at the channel wall along the channel width for the three values of aspect ratio, i.e. approximately similar wall shear stress. On the contrary, the velocity profile along the channel height indicates that the slope of the velocity profile is almost similar for $AR = 0.39$ and 2, i.e. similar wall shear stress and thus similar friction factor. Increasing the aspect ratio beyond 2 resulted in significant changes in the velocity profile as seen for $AR = 10$. The velocity profile became flatter with steep velocity gradient (large slope) near the channel wall, i.e. higher wall shear stress and thus higher friction factor. This may explain why the friction factor increases with aspect ratio for $AR > 2$ in the present study.

Gunnasegaran et al. [17] investigated numerically the effect of geometrical parameters on water flow in multi-microchannel

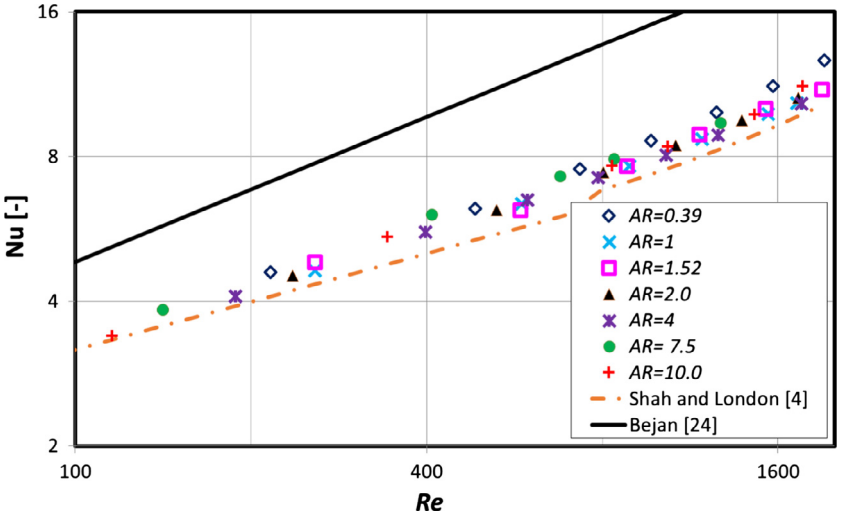

Fig. 15. Comparison between predicted Nusselt number and existing correlations [4,24].

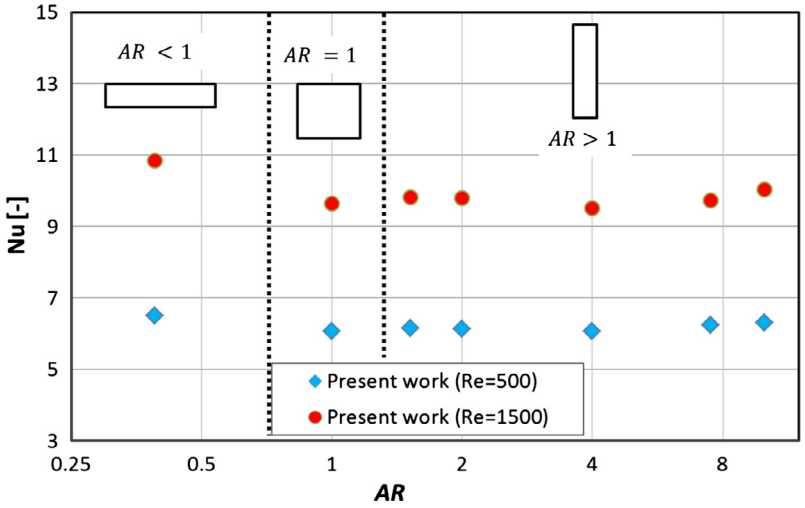

Fig. 16. Variation of Nusselt with varying channel aspect ratio.

configurations. It was reported that the Poiseuille number increases when the ratio W_{ch}/H_{ch} increases (when the aspect ratio decreases). This contradicts the results of the present study, where there is no clear effect of aspect ratio up to $AR = 2$. They attributed the increase of the Poiseuille number with the decrease of aspect ratio to the decrease in flow area and the vortex effects, which become more significant with decreasing aspect ratio. However, inspecting the values of channel depth and width in their study, one can see that increasing the ratio W_{ch}/H_{ch} results in an increase in the flow area, which contradicts their explanation. Fig. 13 depicts the effect of Reynolds number and aspect ratio on the Poiseuille number. The figure demonstrates that the Poiseuille number decreases moderately with *Re* in the very low Reynolds number region then it remains almost unchanged before it increases slightly with *Re* in the high *Re* number region. At low *Re* number, the developing length is very small and the flow becomes fully developed over a significant part of the channel length while at high *Re* number the friction factor increases due to the fact that the flow is developing over a significant part of the channel length. Additionally, it is obvious that the Poiseuille number increases with increasing aspect ratio for $AR > 2$. Xing et al. [27] conducted a theoretical study to investigate the effect of aspect ratio on a fully developed laminar flow in rectangular ducts. Their results showed that the Poiseuille number increases as the aspect ratio decreases, which seems to contradict the results of the present study. It is worth mentioning that the definition of the aspect ratio in their study was such that it was always less than 1 (the ratio of the shortest to the widest side). They gave a simplified equation for the prediction of the friction factor, which is valid for aspect ratio less than 0.2, see Eq. (18) below. For the sake of comparison with this equation, the aspect ratio was defined similarly as [27] and the results of the comparison are shown in Fig. 14. It is clearly shown that there is a good agreement between the results of the present study and the results of [27], i.e. the friction factor increases as the aspect ratio (shortest side/widest side) decreases.

$$Po = \frac{24}{(1+AR)^2(1-0.6274AR)} \tag{18}$$

This initial decrease of Poiseuille number with aspect ratio observed in Fig. 13 was also reported by Kashaninejad et al. [28]. They investigated both analytically and numerically the effects of aspect ratio on friction factor and velocity profile in rectangular microchannels. They reported that the *Po* number decreases sharply from 24 at an aspect ratio near zero to 14.25 at an aspect ratio of 1 as the aspect ratio increases for $AR < 1$. In their study, the

aspect ratio was defined as width to height ratio. For aspect ratios greater than 1, the *Po* increased with increasing aspect ratio until it reached again 24 (the value for parallel plates). Finally, they concluded that $AR \approx 1$, which is a square cross-section channel, generates the lowest friction factor and as the channel cross section deviates from the square shape, the frictional pressure losses increases.

3.2.3. Heat transfer

Fig. 15 shows the average *Nu* plotted versus *Re* for different aspect ratios with the same hydraulic diameter. Also included in the figure are the comparisons with Bejan [24] (Eq. (19)) and Shah and London [4] Eq. (20) correlations for hydrodynamically developed and thermally developing flow.

$$Nu = 1.375\left(\frac{L}{RePrDh}\right)^{-0.5} \tag{19}$$

$$Nu = 1.953(RePrDh/L)^{1/3}; \left(\frac{RePrDh}{L}\right) \geqslant 33.3 \tag{20.a}$$

$$Nu = 4.364 + 0.0722(RePrDh/L); \left(\frac{RePrDh}{L}\right) < 33.3 \tag{20.b}$$

It is obvious that the average Nusselt number increases with *Re*, which indicates that the flow is thermally developing, bearing in mind that the flow is laminar. Also, the aspect ratio effect on *Nu* is insignificant. Additionally, the results agree reasonably well with the correlation of Shah and London with values that are slightly higher. The correlation of Bejan [24], however, over predicts the data significantly. In order to clarify the effects of aspect ratio, the data of Fig. 15 were plotted in Fig. 16 as average *Nu* versus aspect ratio for *Re* = 500 and 1500. As shown in Fig. 16, the channels were classified into shallow channel ($AR < 1$), square channel ($AR = 1$) and deep channel ($AR > 1$). The figure shows that the

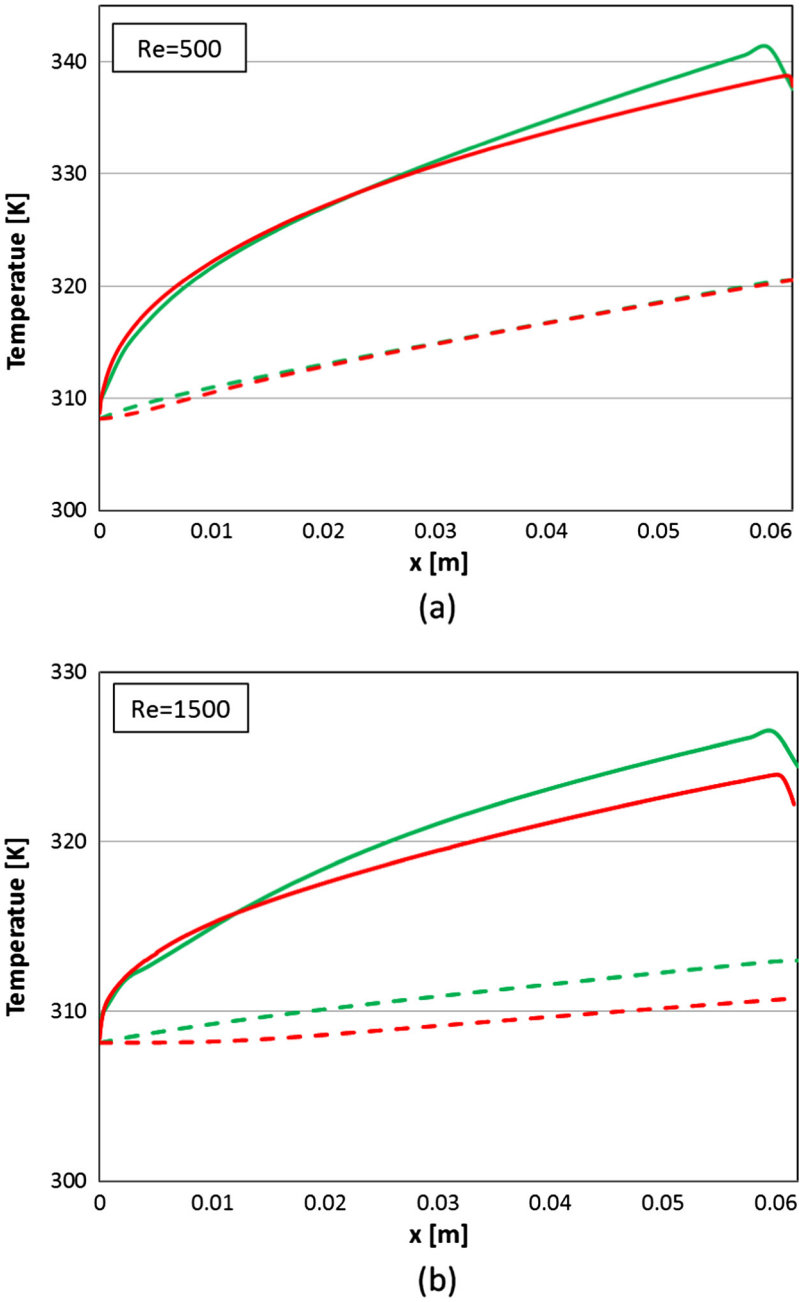

Fig. 17. Comparison of wall temperature (solid line) and fluid temperature (dotted line) for tested aspect ratio at (a) $Re \approx 500$ (b) $Re \approx 1500$; [red] $AR = 0.39$; [green] $AR = 10$.

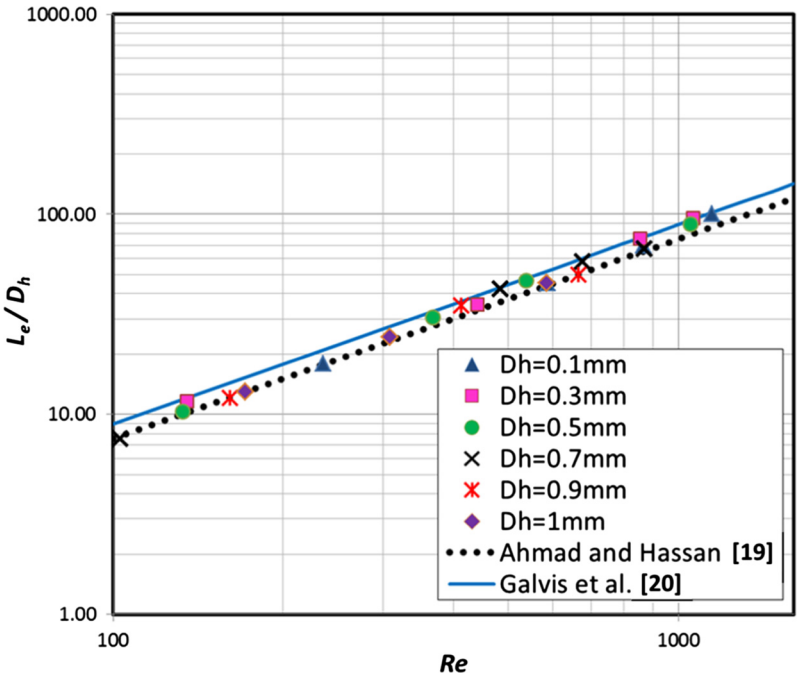

Fig. 18. Comparison of obtained dimensionless entrance length at different channel hydraulic diameter ($0.1 < D_h$ (mm) < 1) with existing correlations. [19,20].

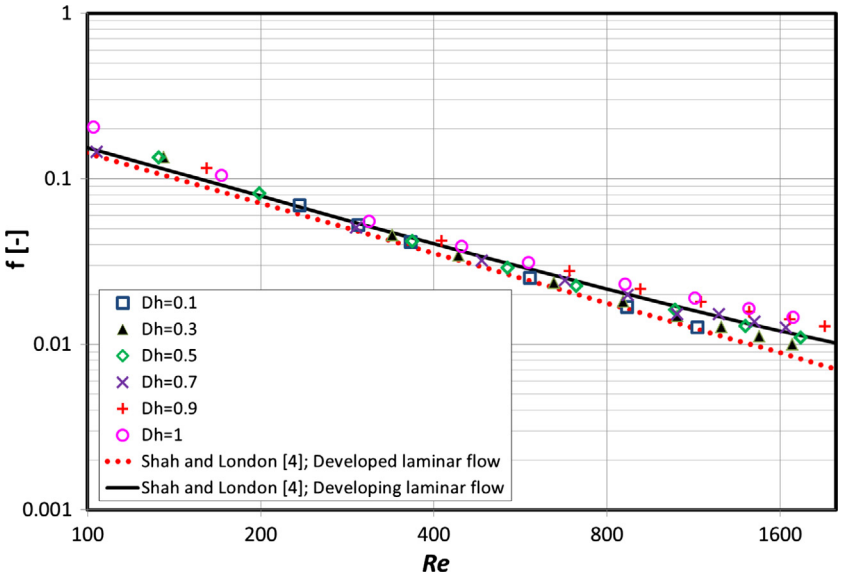

Fig. 19. Comparison between predicted friction factor and existing correlations [4].

effect of aspect ratio on the average Nusselt number is insignificant. It is worth mentioning that a constant heat flux value was applied at the bottom and side walls of all tested channels and the hydraulic diameter was kept constant. Thus, the insignificant effect of aspect ratio on heat transfer rates in this study could be attributed to the behaviour of the wall and fluid temperature. Fig. 17a and b depicted the fluid and wall temperature distribution along the channel for $Re = 500$ and $Re = 1500$, respectively and for the lowest and highest aspect ratio. It is clearly shown that the temperature difference between the wall and fluid temperature is almost the same for the two channels. Therefore, the Nu values at a given Re number showed insignificant deviation for all cases. The results obtained in this study agree with Harm et al. [29] who reported that the effect of aspect ratio on heat transfer rates is insignificant.

3.3. Effect of hydraulic diameter

In this section, the effect of hydraulic diameter was studied by varying D_h between 0.1 and 1 mm while the aspect ratio was kept constant at $AR = 1$. The dimensionless entrance length for all tested microchannels was compared with existing correlations [19,20] and was depicted in Fig.18. Similar conclusions can be drawn as in Section 3.2, as the dimensionless entrance length was observed to become independent of hydraulic diameter and the results were found to agree well with Ahmad and Hassan [19]. In Fig. 19, the friction factor data are plotted against Re and compared with existing correlations [4]. The figure shows that the friction factor is in a reasonable agreement with Shah and London [4] and no clear effect of the hydraulic diameter on the friction factor could be identified. The friction factor at $Re = 500$ and

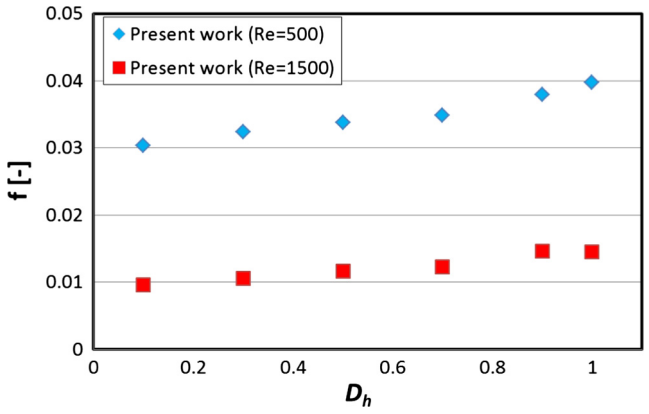

Fig. 20. Variation of friction factor with varying channel hydraulic diameter, D_h.

Re = 1500 is plotted against the hydraulic diameter in Fig. 20 in order to clarify the effect of hydraulic diameter. Fig. 20 shows that the friction factor increases with increasing hydraulic diameter, which agrees with the results of Peng et al. [2] and Xu et al. [5], but contradicts the findings of some researchers [6,10,27] who reported an insignificant effect of hydraulic diameter on the friction factor. The friction factor in the present study increased by 22.94 % for *Re* = 500 and increased by 32.53% for *Re* = 1500 when the hydraulic diameter increased from 0.1 mm to 1 mm. Silverio and Moreira [30] studied the pressure drop and heat transfer in fully developed flow in channels with square and circular cross section with hydraulic diameter ranging from 0.05 mm to 0.5 mm. Three different working fluids were used: distilled water, methoxy-nonafluorobutane and methanol. They stated that the microscale effect is negligible in channels with a hydraulic diameter larger than 0.2 mm and for smaller channels the results were found to deviate from the classical theory at *Re* < 100. In order to explain the effect of hydraulic diameter in the present study, the fully developed velocity profile along the channel width and height were plotted in Fig. 21, at *Re* = 500 and 1500 and for D = 0.1, 0.5 and 1 mm. The figures demonstrate that the velocity profile plotted along the channel width and height is very similar with insignificant changes as the hydraulic diameter increases. The similarity of the velocity profile along the channel width and height arises from the fact that all examined channels have a square cross sectional area (*AR* = 1). This similarity in the velocity profile leads to the conclusion that the local wall shear stress and thus the local friction factor values are similar in the fully developed region irrespective of the value of the hydraulic diameter. Accordingly, the increase of friction factor with hydraulic diameter found in the present study cannot be explained using the velocity profile and shear stress. The reason could be attributed to the increase of the hydrodynamic entry length (the dimensional value) with increasing the hydraulic diameter and Reynolds number. As the length of the entry region increases, the average pressure drop and thus the average friction factor increases.

The effect of hydraulic diameter on Nusselt number was illustrated in Fig. 22. As seen in the figure, the Nusselt number increases with *Re* as expected and the numerical values agree reasonably well with the predicted values using the correlation of Bejan [24] for the whole diameter range except D_h = 0.1 mm, where a significant deviation was observed. The effect of the hydraulic diameter on *Nu* is clearly shown in Fig. 23 for *Re* = 500 and 1500 compared to the predictions from Shah and London [4]. As seen

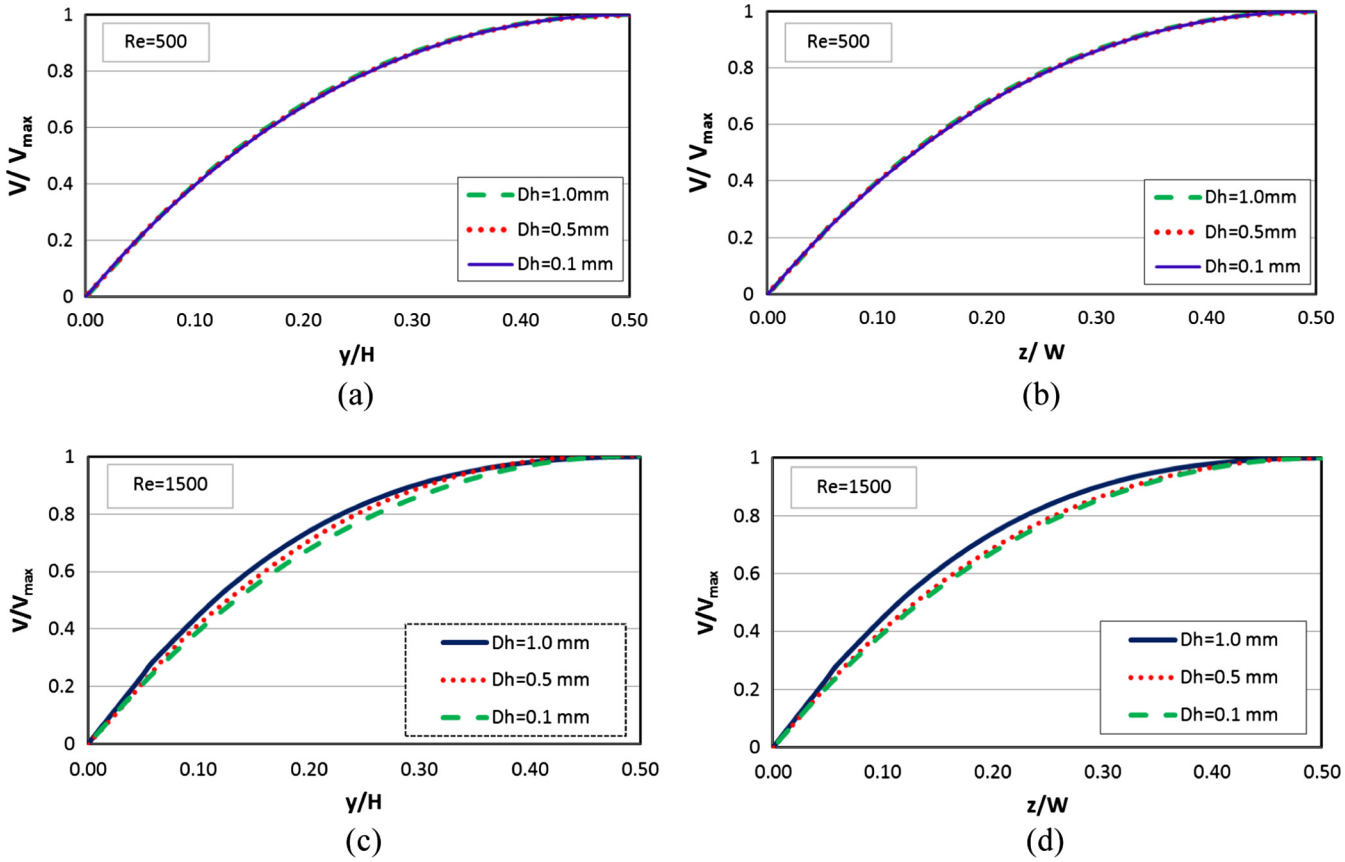

Fig. 21. Fully developed velocity profile against channel height and width microchannel for D_h = 0.1 mm, 0.5 mm and 1 mm at *Re* ≈ 500 and *Re* ≈ 1500.

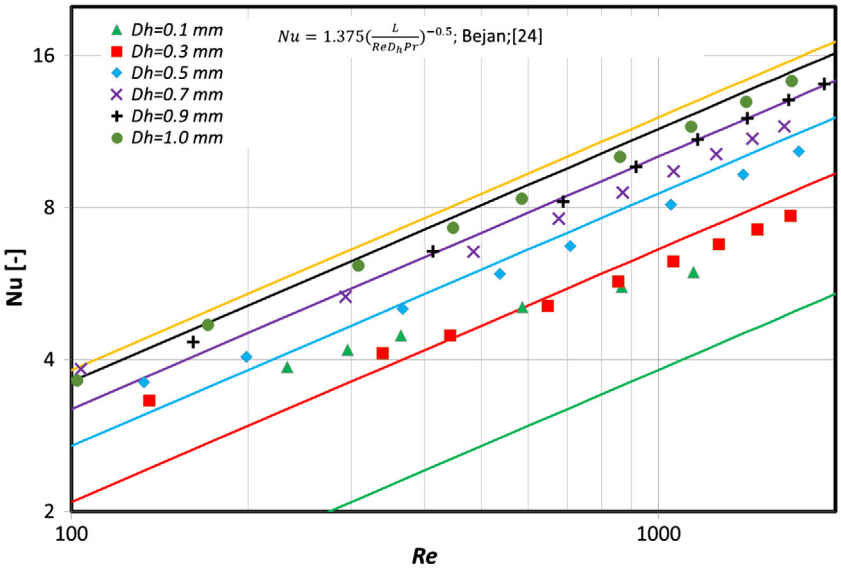

Fig. 22. Comparison between numerical Nusselt number predictions and existing correlation [25] (solid line; [orange] 1 mm; [**black**] 0.9 mm; [purple] 0.7 mm; [blue] 0.5 mm; [red] 0.3 mm; [green] 0.1 mm) with varying channel hydraulic diameter.

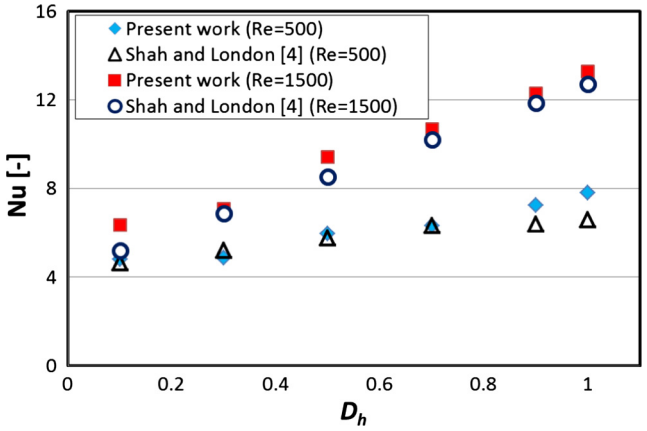

Fig. 23. Variation of Nusselt with varying hydraulic diameter.

in Fig. 23, the hydraulic diameter affects significantly the average Nusselt number where *Nu* increases with increasing hydraulic diameter. This phenomenon is further explained below. Also, the figure demonstrates that the numerical data are in excellent agreement with the predictions using the Shah and London [4] correlation. Fig. 24 shows the wall and fluid temperature at $Re = 500$ and $Re = 1500$ for the lowest and highest D_h tested in this study in order to explain the effect of the hydraulic diameter. The figure indicates that the temperature difference between wall and fluid for $D_h = 1$ mm is higher compared to $D_h = 0.1$ mm. Therefore, the magnitude of the dimensional heat transfer coefficient for $D_h = 0.1$ mm is higher compared to $D_h = 1$ mm. In other words, the dimensional heat transfer coefficient increases as the hydraulic diameter decreases. On the contrary, Fig. 23 depicts an opposite effect for hydraulic diameter on Nusselt number. This is arising from the fact that the Nusselt number depends on two variables namely the hydraulic diameter and the heat transfer coefficient ($Nu = hD_h/k$). Since the heat transfer coefficient (h) decreases as D_h increases, the value of *Nu* will depend on which variable has a more dominant effect. Fig. 25 clarifies this point by plotting the local heat transfer coefficient and *Nu* against the axial distance for $D_h = 0.1$–1 mm and $Re = 500$ and 1500. The figure shows clearly that the local heat transfer coefficient increases with decreasing hydraulic diameter while the opposite occurs for *Nu*. Also, the figure shows that for $Re = 500$ the flow is thermally developing for all diameters except for $D_h = 0.1$ where the values reached almost a constant value. The same result was found in the numerical work of Lee and Garimella [31] for laminar, thermally developing flow in microchannels having a hydraulic diameter and an aspect ratio range between 200 to 364 μm and 1 to 10, respectively. The local and average Nusselt numbers showed a decrease with decreasing hydraulic diameter and increasing aspect ratio. Dharaiya and Kandlikar [16] also studied the effect of aspect ratio, ranging from 0.1 to 10, in a rectangular microchannel. The hydraulic diameter varied as the aspect ratio changed. So from this study it is difficult to determine which geometric parameter has the most significant effect on heat transfer. It is interesting to note that the predicted *Nu* for fully developed flow obtained in five different cases showed an inconsistent trend for each tested case. In this present study, the average *Nu* number increased with increasing hydraulic diameter and followed the same trend as found for the one heated-wall boundary-condition presented by Dharaiya and Kandlikar [16]. As shown in the sections above, the present results indicate that the hydraulic diameter has the most significant effect on heat transfer while the effect of the aspect ratio on heat transfer at a given hydraulic diameter is negligible. Furthermore, as shown in Fig. 23, the present results were found to be in a good agreement with the correlation of Shah and London [4] for all the range studied.

4. Effect of channel geometry on entry/exit losses

In most experimental studies that include inlet/outlet restrictions, the channel pressure drop was estimated by subtracting all minor losses (sudden contraction and enlargement) from the total measured pressure drop. The minor losses were calculated using equations proposed for large geometries, implicitly assuming that the flow structure would be the same in micro geometries. In the present study, the minor losses were examined in order to assess whether they can be ignored or not. Fig. 26 shows the pressure variation along the test section from the mid plane of the inlet plenum to the mid plane of the outlet plenum. It is obvious that there

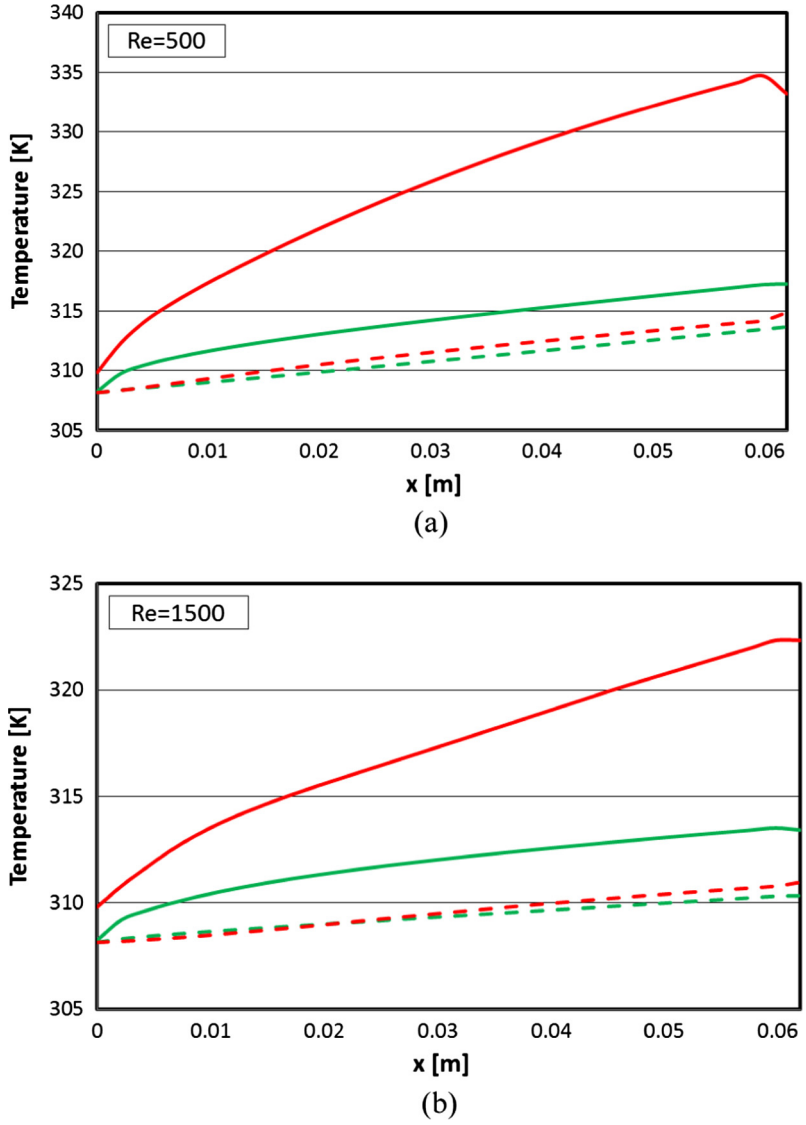

Fig. 24. Comparison of wall temperature (solid line) and fluid temperature (dotted line) for tested aspect ratio at (a) $Re \approx 500$ (b) $Re \approx 1500$; [red] $D_h = 1$ mm; [green] $D_h = 0.1$ mm.

is a sudden decrease in pressure from the inlet plenum to the channel inlet due to the 90° change in flow direction, further downstream the pressure decreases linearly up to the channel exit where a sudden increase occurs due to pressure recovery in the outlet plenum. Also, the small pressure recovery due to vena contracta at the channel inlet is not observed, i.e. there were negligible losses due to the sudden contraction. The entry and exit losses (combined losses due to change in flow direction and change in flow area) are estimated in the present study and the values are summarized in Table 2. As mentioned in Section 2, a uniform velocity was employed at the inlet plenum. Differences in channel area, however, resulted in different velocities in the channel. Therefore, a *Re* number between 520 and 677 was chosen in order to compare the entry and exit losses for all tested channels. The table demonstrates that the entry losses ranged from 7.33% to 10.51% for $AR = 0.39–10$ and $D_h = 0.56$ mm and ranged from 2.37% to 14.19% for $D_h = 0.1–1$ mm and $AR = 1$. The exit losses ranged from 1.96% to 22.35% for $AR = 0.39–1$ and ranged from 1.36 to 29.67 for $D_h = 0.1–1$ mm. This means that regardless of the geometrical parameter (aspect ratio or hydraulic diameter) the entry and exit losses could be significant and should be taken into consideration. In the last two columns of Table 2, the numerical values were compared with the values predicted using conventional macroscale equations given below for sudden expansion, sudden contraction and 90° changes in flow direction. These Eqs. (21)–(23) are taken from Ref. [32]. For the entry losses, the numerical values were lower by 6.7–22% compared to the prediction using the conventional equations. For the exit losses the difference was significant where the numerical values were 28–45% lower. In conclusion, using the conventional equations for predicting the minor losses in microchannels could result in significant error in the calculations of the experimental friction factor and thus caution should be exercised when comparing with the laminar flow theory.

The sudden expansion losses are calculated by:

$$\Delta p_{ex} = \left(1 - \frac{A_{ch}}{A_p}\right)^2 \times \frac{1}{2}\rho V_{ch}^2 \tag{21}$$

For sudden contraction, the contraction losses are defined using a loss coefficient K_c as given in Eq. (20). The value of this coefficient ranges from 0 to 0.5 depending on the small to large area ratio (A_{ch}/A_p), which is given in [26] in the form of a chart.

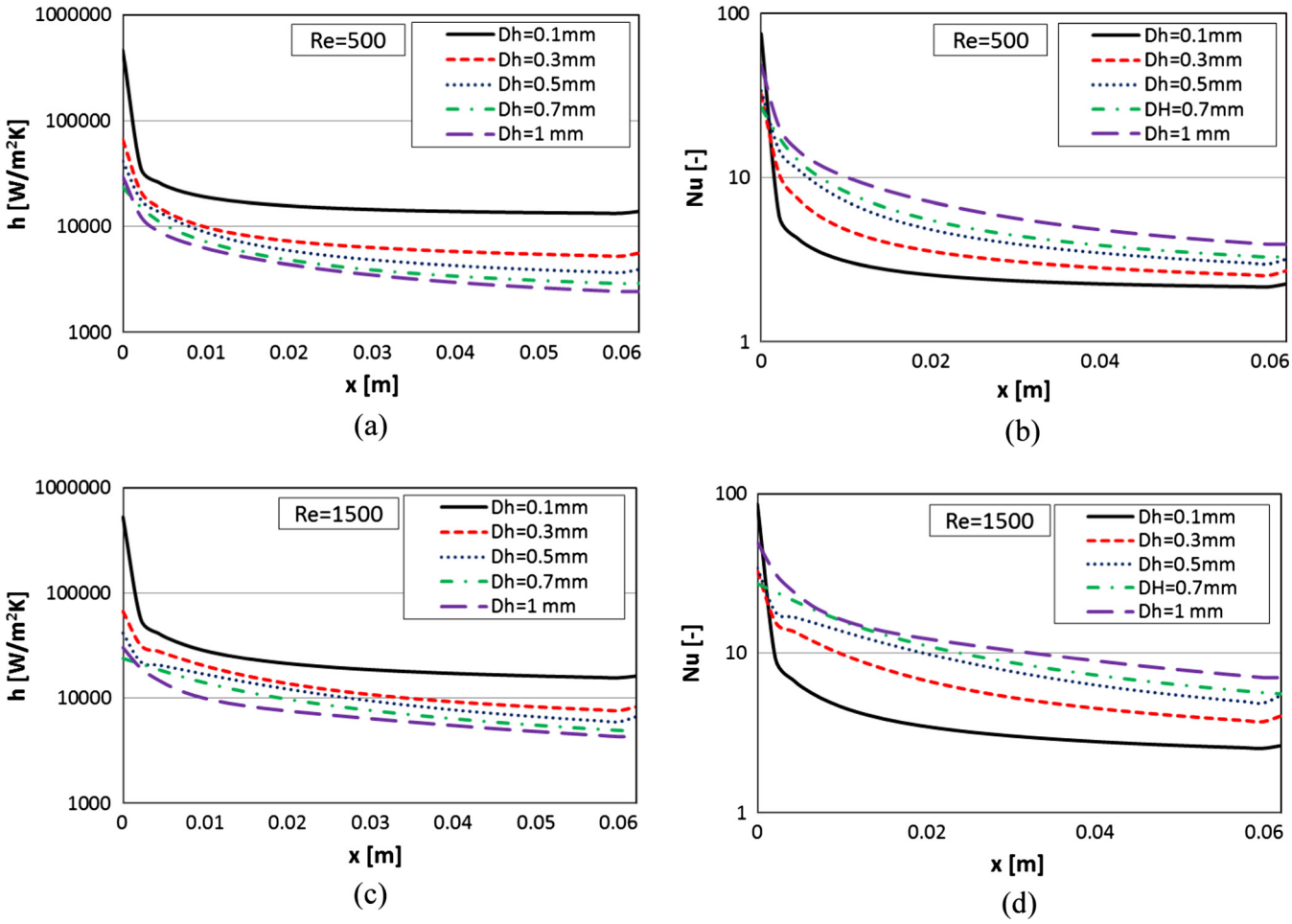

Fig. 25. Axial heat transfer coefficient and Nusselt number at *Re* = 500 (a and b) and *Re* 1500 (c and d).

$$Deltap_c = K_c \times \frac{1}{2}\rho V_{ch}^2 \tag{22}$$

For a sharp change in flow direction by 90°, the following equation was used:

$$\Delta p_{90} = K_{90} \times \frac{1}{2}\rho V_p^2, \quad K_{90} = 1.1 \tag{23}$$

5. Thermal performance index (TPI)

The thermal performance index defined in [33] as the ratio between the heat exchanger effectiveness (ratio of the actual heat transfer rate to the maximum possible heat transfer rate) and pressure drop is a useful mean for the evaluation of heat exchangers. In this study, only single channel was investigated rather than a complete microchannel heat exchanger. However, the same principle can be applied to evaluate the effect of hydraulic diameter and aspect ratio on the thermal-hydraulic performance. Thus the thermal performance index is defined in this study as:

$$\xi = \frac{\dot{m}c_p(T_{out} - T_{in})}{q'' A_{ht}\Delta p} \tag{24}$$

where $\dot{m}$ is mass flow rate and A_{ht} is the total heat transfer area, $(W + 2H)L$. Fig. 27a depicts the effect of aspect ratio on the performance index while Fig. 27b shows the effect of hydraulic diameter. Both figures indicate that the performance index decreases with increasing Reynold number. The aspect ratio did not affect the performance index significantly for AR > 1 while the performance index was higher for AR = 0.39 compared to the other values of aspect ratio. Fig. 27b indicated a clear effect for the hydraulic diameter where the performance index was higher for larger diameter at the same Reynolds number. The conclusion based on the performance index is different from the conclusion based on the separate analysis of friction factor. For example, it was concluded that, based on the friction factor data only, channels with aspect ratio between 1 and 2 is recommended to achieve low pressure drop. On the contrary, including the heat transfer in the evaluation using the ther-

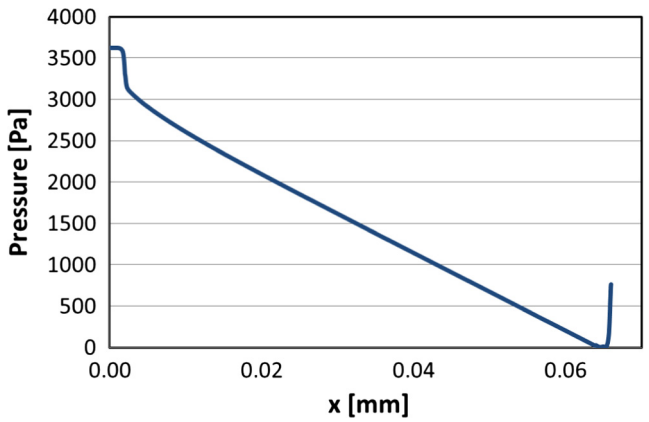

Fig. 26. The pressure along the test section for *Re* = 578, D_h = 0.56 mm, *AR* = 1.52.

Table 2
Entry and exit pressure losses.

Run	*AR*	D_h (mm)	*Re*	ΔP_{total} (Pa)	$\Delta P_{entry,num}$ (%)	$\Delta P_{exit,num}$ (%)	$\frac{\Delta P_{entry,num}}{\Delta P_{entry,con}}$	$\frac{\Delta P_{exit,num}}{\Delta P_{exit,con}}$
1	0.39	0.56	657	5191.99	10.51	10.68	0.933	0.610
2	1	0.56	585	3635.64	9.65	22.35	0.844	0.597
3	1.52	0.56	600	3491.38	10.07	13.25	0.892	0.598
4	2	0.56	520	3327.79	7.74	16.46	0.787	0.604
5	4	0.56	574	4310.94	7.38	5.29	0.777	0.628
6	7.5	0.56	637	5325.94	7.77	1.96	0.822	0.678
7	10	0.56	637	5540.39	7.33	1.97	0.813	0.714
8	1	0.1	586	528469.00	2.37	1.36	0.902	0.547
9	1	0.3	648	23783.50	6.24	10.07	0.787	0.560
10	1	0.5	537	4523.58	8.09	16.31	0.788	0.586
11	1	0.7	677	2537.00	12.88	29.67	0.827	0.628
12	1	0.9	666	1168.85	14.19	28.65	0.850	0.685
13	1	1	585	766.77	13.99	27.83	0.876	0.721

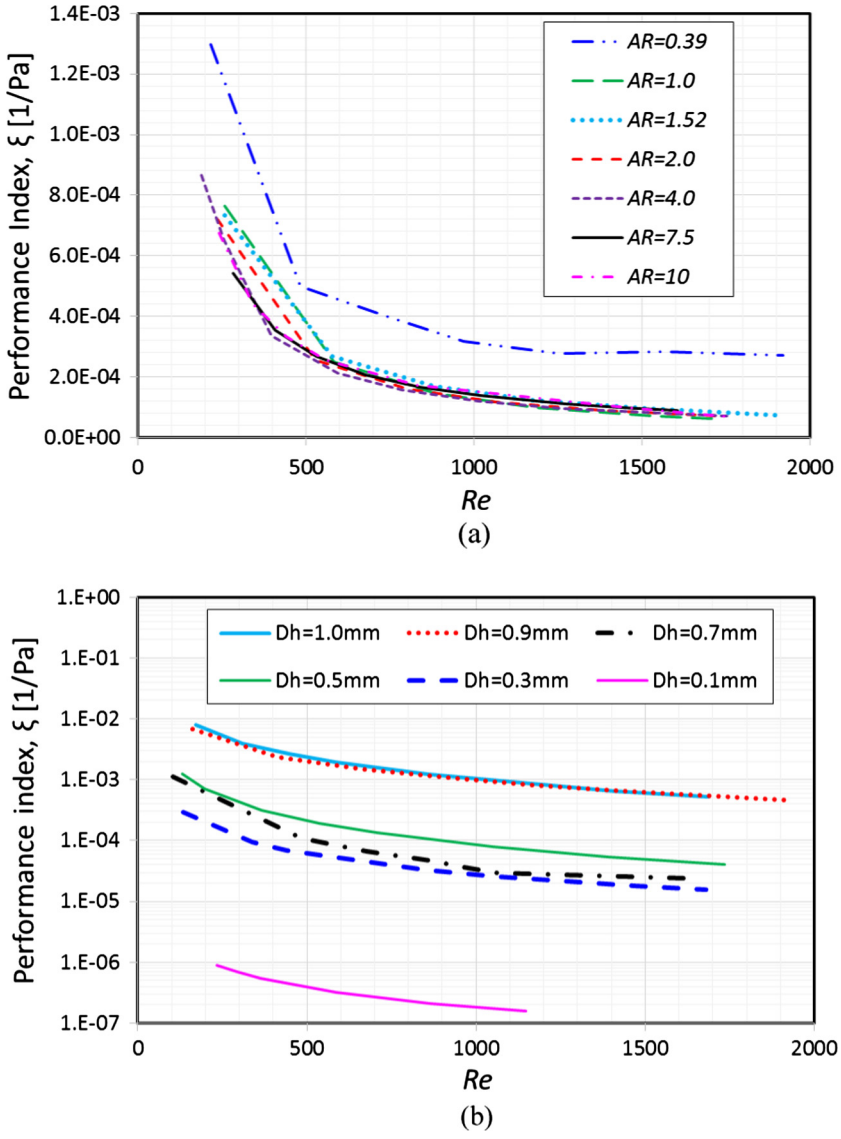

Fig. 27. Variation of thermal performance index against *Re* at difference (a) *AR* and (b) D_h

mal performance index, a channel with aspect ratio 0.39 gave the highest performance. This means that the performance index should be included for the analysis of thermal-hydraulic performance of microchannels heat exchangers.

6. Conclusions

Numerical simulations were carried out to investigate the effect of hydraulic diameter and aspect ratio on fluid flow and heat trans-

fer in single rectangular microchannels. In the simulations, a constant heat flux boundary condition was applied on three walls, while the fourth top wall was adiabatic. In the first set of simulations, the range of hydraulic diameters was varied from 0.1 to 1 mm and the aspect ratio was fixed at 1. In the second set of simulations, the aspect ratio was varied between 0.39 and 10 while the hydraulic diameter was kept constant at 0.56 mm. The simulations were conducted for a range of Reynolds number from 100 to 2000 (laminar flow) and water was used as the working fluid. Entrance and exit effects were considered by including inlet/outlet plenums. The following conclusions can be drawn:

1. The dimensionless hydrodynamic entrance length does not depend on aspect ratio and hydraulic diameter. The correlations given by Ahmad and Hassan [19] and Galvis et al. [20] can predict reasonably the hydrodynamic entry length.
2. The friction factor was found to decrease slightly with increasing aspect ratio (AR) until $AR \approx 2$ after which it increases continuously with aspect ratio. Thus, based on friction factor data only, an aspect ratio between 1 and 2 may be recommended for design in order to achieve low pressure drop. However, including heat transfer and using the thermal performance index as an evaluation criterion, channels with $AR = 0.39$ gave the best performance.
3. Increasing the aspect ratio beyond 2 resulted in a significant effect on the velocity profile. It changed from a nearly parabolic shape at low aspect ratio to a flattened shape with a large slope at high aspect ratio. This may explain why the friction factor increases with aspect ratio.
4. The aspect ratio has an insignificant effect on the heat transfer rate.
5. The friction factor and average Nusselt number increases with increasing hydraulic diameter for simultaneously thermally and hydrodynamically developing flow.
6. The effect of the hydraulic diameter on friction factor and heat transfer is more important compared to the effect of aspect ratio.
7. The correlations of Shah and London [4] for predictions of friction factor and heat transfer rates are still applicable at micro scale with a reasonable accuracy. This agrees with the conclusion given by Rosa et al. [10] who reported that macro scale theory and correlations are valid at micro scale if measurement uncertainty and scaling effects were carefully considered.
8. The simultaneous variation in hydraulic diameter and aspect ratio encountered in previous experimental studies is not a reason for the deviation from the macro scale theory reported in these studies.
9. The thermal performance index should be taken into consideration in the analysis of thermal-hydraulic performance of microchannels heat exchangers.

References

[1] X.F. Peng, G.P. Peterson, The effect of thermofluid and geometrical parameters on convection of liquids through rectangular microchannels, Int. J. Heat Mass Transfer 38 (4) (1995) 755–758.
[2] X.F. Peng, G.P. Peterson, B.X. Wang, Frictional flow characteristics of water flowing through rectangular microchannels, Exp. Heat Transfer 7 (4) (1994) 249–264.
[3] D. Pfund, D. Rector, A. Shekarriz, A. Popescu, J. Welty, Pressure drop measurements in a microchannel, AIChE J. 46 (8) (2000) 1496–1507.
[4] R.K. Shah, A. London, Laminar flow forced convection in ducts, in: T.F. Irvine, J. P. Hartnett (Eds.), Advances in Heat Transfer (Suppl. 1), Academic Press, New York, 1978.
[5] B. Xu, K. Ooti, N. Wong, W. Choi, Experimental investigation of flow friction for liquid flow in microchannels, Int. Commun. Heat Mass Transfer 27 (8) (2000) 1165–1176.
[6] P. Gao, S. Le Person, M. Favre-Marinet, Scale effects on hydrodynamics and heat transfer in two-dimensional mini and microchannels, Int. J. Therm. Sci. 41 (11) (2002) 1017–1027.
[7] J. Zhang, Y. Diao, Y. Zhao, Y. Zhang, An experimental study of the characteristics of fluid flow and heat transfer in the multiport microchannel flat tube, Appl. Therm. Eng. 65 (2014) 209–218.
[8] J. Judy, D. Maynes, B. Webb, Characterization of frictional pressure drop for liquid flows through microchannels, Int. J. Heat Mass Transfer 45 (17) (2002) 3477–3489.
[9] O. Mokrani, B. Bourouga, C. Castelain, H. Peerhossaini, Fluid flow and convective heat transfer in flat microchannels, Int. J. Heat Mass Transfer 52 (5–6) (2009) 1337–1352.
[10] P. Rosa, T. Karayiannis, M. Collins, Single-phase heat transfer in microchannels: the importance of scaling effects, Appl. Therm. Eng. 29 (17–18) (2009) 3447–3468.
[11] G. Gamrat, M. Favre-Marinet, D. Asendrych, Conduction and entrance effects on laminar liquid flow and heat transfer in rectangular microchannels, Int. J. Heat Mass Transfer 48 (14) (2005) 2943–2954.
[12] R.K. Shah, D.P. Sekulic, Fundamentals of Heat Exchanger Design, John Willey and Sons, Inc., 2003.
[13] P. Lee, S. Garimella, D. Liu, Investigation of heat transfer in rectangular microchannels, Int. J. Heat Mass Transfer 48 (9) (2005) 1688–1704.
[14] A. Sahar, M. Özdemir, E. Fayyadh, J. Wissink, M. Mahmoud, T. Karayiannis, Single phase flow pressure drop and heat transfer in rectangular metallic microchannels, Appl. Therm. Eng. 93 (2016) 1324–1336.
[15] M.K. Moharana, S. Khandekar, Effect of aspect ratio of rectangular microchannels on the axial back conduction in its solid substrate, Int. J. Microsc. Nanosc. Thermal Fluid Transport Phenom. 4 (2012) 211–229.
[16] V. Dharaiya, S. Kandlikar, Numerical investigation of heat transfer in rectangular microchannels under H2 boundary condition during developing and fully developed laminar flow, J. Heat Transfer 134 (2) (2012) 020911.
[17] P. Gunnasegaran, H. Mohammed, N. Shuaib, R. Saidur, The effect of geometrical parameters on heat transfer characteristics of microchannels heat sink with different shapes, Int. Commun. Heat Mass Transfer 37 (8) (2010) 1078–1086.
[18] H. Wang, Z. Chen, J. Gao, Influence of geometric parameters on flow and heat transfer performance of micro-channel heat sinks, Appl. Therm. Eng. 107 (2016) 870–879.
[19] T. Ahmad, I. Hassan, Experimental analysis of microchannel entrance length characteristics using microparticle image velocimetry, J. Fluids Eng. 132 (4) (2010) 041102.
[20] E. Galvis, S. Yarusevych, J. Culham, Incompressible laminar developing flow in microchannels, J. Fluids Eng. 134 (1) (2012) 014503.
[21] A.G. Fedorov, R. Viskanta, Three-dimensional conjugate heat transfer in the microchannel heat sink for electronic packaging, Int. J. Heat Mass Transfer 43 (2000) 399–415.
[22] W. Qu, I. Mudawar, Experimental and numerical study of pressure drop and heat transfer in a single-phase microchannel heat sink, Int. J. Heat Mass Transfer 45 (2002) 2549–2565.
[23] M.R. Ozdemir, M.M. Mahmoud, T.G. Karayiannis, Flow boiling heat transfer in rectangular copper microchannel, in: International Conference on Advances in Mechanical Engineering Istanbul, Turkey 2015-ICAME'15, 13–15 May 2015, Yildiz Technical University, 2015.
[24] A. Bejan, Convection Heat Transfer, John Wiley and Son, Inc., New Jersey, 2004.
[25] W. Qu, I. Mudawar, S.Y. Lee, S.T. Wereley, Experimental and computational investigation of flow development and pressure drop in a rectangular microchannel, J. Electron. Pack. 128 (1) (2006) 1–9.
[26] G. Beavers, E. Sparrow, R. Magnuson, Experiments on hydrodynamically developing flow in rectangular ducts of arbitrary aspect ratio, Int. J. Heat Mass Transf. 13 (4) (1970) 689–701.
[27] D. Xing, C. Yan, C. Wang, L. Sun, A theoretical analysis about the effect of aspect ratio on single-phase laminar flow in rectangular ducts, Prog. Nucl. Energy 65 (2013) 1–7.
[28] N. Kashaninejad, W.K. Chan, N.-T. Nguyen, Analytical and numerical investigations of the effects of microchannel aspect ratio on velocity profile and friction factor, in: International Conference on Computational Method, Gold Coast, Australia, 2012.
[29] T. Harms, M. Kazmierczak, F. Gerner, Developing convective heat transfer in deep rectangular microchannels, Int. J. Heat Fluid Flow 20 (2) (1999) 149–157.
[30] V. Silvério, A.L. Moreira, Friction losses and heat transfer in laminar microchannel single-phase liquid flow, in: Proceedings of 6th International ASME Conference on Nanochannels, Microchannels and Minichannels, Darmstadt, German, 2008.
[31] P.S. Lee, S.V. Garimella, Thermally developing flow and heat transfer in rectangular microchannels of different aspect ratios, Int. J. Heat Mass Transfer 49 (17–18) (2006) 3060–3067.
[32] B.R Munson, D.F. Young, T.H. Okiishi, W.W. Huebsch, Fundamentals of Fluid Mechanics, sixth ed., John Willey and Sons, Inc., 2009.
[33] M.I. Hassan, A.M.A. Rageb, M. Yaghoubi, Investigation of counter current flow microchannel heat exchanger performance with using nanofluid as a coolant, J. Electron. Cool. Thermal Control 2 (2012) 35–43.